Hydrothermal Synthesis of Delafossite-Type Oxides

William C. Sheets, Emmanuelle Mugnier, Antoine Barnabé, Tobin J. Marks, Kenneth R. Poeppelmeier

Hydrothermal Synthesis of Delafossite-Type Oxides

William C. Sheets,[†] Emmanuelle Mugnier,[‡] Antoine Barnabé,[‡] Tobin J. Marks,[†] and Kenneth R. Poeppelmeier*[,†]

Department of Chemistry, Northwestern University, Evanston, Illinois 60208-3113, and Laboratoire LCMIE/CIRIMAT CNRS UMR 5085, Université Paul Sabatier Toulouse III, 118 Route de Narbonne, 31062 Toulouse Cedex, France

The syntheses of copper and silver delafossite-type oxides from their constituent binary metal oxides, oxide hydroxides and hydroxides, by low temperature (<210 °C) and low pressure (<20 atm) hydrothermal reactions are described. Particular emphasis is placed on how the acid−base character of a constituent oxide determines its solubility and therefore whether a particular delafossite-type oxide can be synthesized, a strategy utilized by geologists and mineralogists to understand the conditions necessary for the synthesis of various minerals. Thus, the geochemical and corrosion science literature are shown to be useful in understanding the reaction conditions required for the syntheses of delafossite-type oxides and the relationship between reactant metal oxide acid−base character, solubility, aqueous speciation, and product formation. Manipulation of the key parameters, temperature, pressure, pH, and reactant solubility, results in broad families of phase-pure delafossite-type oxides in moderate to high yields for copper, $CuBO_2$ (B = Al, Sc, Cr, Mn, Fe, Co, Ga, and Rh), and silver, $AgBO_2$ (B = Al, Sc, Fe, Co, Ni, Ga, Rh, In, and Tl).

1. Introduction

Delafossite, a copper and iron oxide mineral, was first reported by Friedel in 1873 and named in honor of the French mineralogist and crystallographer, Gabriel Delafosse.[1] First confirmed by Pabst[2] as having the same structure as synthetic $CuFeO_2$,[3] the delafossite structure is constructed from alternate layers of two-dimensional close-packed copper cations with linear $O-Cu^+-O$ bonds and slightly distorted edge-shared $Fe^{3+}O_6$ octahedra. Furthermore, each oxygen is coordinated by four cations (one Cu^+ and three Fe^{3+}). Delafossites can crystallize in either a rhombohedral 3R- ($R\bar{3}m$) or hexagonal 2H- ($P6_3/mmc$) polytype based on the stacking of the alternating layers,[4,5] Figure 1. This structure type maintains the expected valences for the monovalent A-site cations (Ag^+, Cu^+, Pd^+, and Pt^+) and trivalent B-site cations ($0.53 < r(B^{3+}) < 1.03$ Å).[6,7] Recently, owing to their application as catalysts,[8−12] luminescent materials,[13,14] batteries,[15] and transparent *p*-type conducting oxides,[16−18] delafossite-type oxides have been studied intensely. The specific cation combination for each delafossite-type oxide determines its application. The A-site cations, Cu^+ and Ag^+ (d^{10} ions), are more appropriate for enhanced optical transparency, while formal Pd^+ and Pt^+ (d^9 ions)[19,20] are better choices for improved electrical conductivity. Owing to the optical absorption from d−d electron transitions, trivalent B-site cations suitable for transparency must possess empty or closed d-electron shells (groups 3 and 13), while partially filled d-electron shells (transition metals) find application in batteries and catalysis.

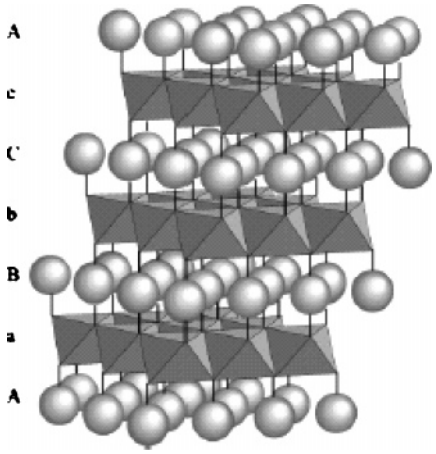

Figure 1. Schematic representation of the delafossite structure (ABO_2) for the "3R" polytype ($R3m$) with AaBbCcAa... stacking along the *c*-axis. The "2H" polytype ($P6_3/mmc$) has an alternate AaBbAa... stacking sequence. The polyhedra and spheres represent $B^{3+}O_6$ distorted octahedra and linearly coordinated A^+ cations, respectively.

The simple binary oxides of the noble elements palladium (PdO), platinum (PtO_2), and silver (Ag_2O) decompose in air at the temperatures of 800, 650, and 300 °C, respectively, because of their low free energies of formation. As a result, while delafossite-type oxides with copper on the A-site can be synthesized readily by high-temperature solid-state reactions, those with the noble metals containing palladium, platinum, or silver are difficult to prepare in a single step

* To whom correspondence should be addressed. E-mail: krp@northwestern.edu.
[†] Northwestern University.
[‡] Université Paul Sabatier Toulouse III.

10.1021/cm051791c

by solid-state syntheses because these oxides decompose in open reaction systems before an appreciable reaction can occur.[21] To a certain degree, the difficulty normally encountered in the synthesis of mixed metal oxides of palladium, platinum, and silver, specifically the delafossite-type oxides, has been overcome using low-temperature and/or closed reaction systems. For example, the first polycrystalline silver delafossite-type oxide, silver ferrate ($AgFeO_2$), was prepared at low temperatures (100 °C) by Krause from the combination of a "meta-ferric hydroxide gel" (γ-FeOOH) and Ag_2O in a boiling NaOH solution.[22] To prepare small single crystals, Croft, Tombs, and England employed thin-walled platinum tubes at higher temperatures (400 °C) and pressures (2700 atm) to synthesize $AgFeO_2$ from Ag_2O and Fe_2O_3 and therefore took advantage of a closed system (hydrothermal conditions) to prevent decomposition of the Ag_2O.[23] Later, Shannon, Rogers, and Prewitt reported the first comprehensive study of three closed system syntheses (metathetical, oxidizing flux, and hydrothermal) to generate numerous single crystal and powder examples of the four different classes of delafossite-type oxides, each incorporating a different A-site cation: $CuBO_2$ (B = Al, Fe, Co, Ga, and Rh), $AgBO_2$ (B = Cr, Fe, Co, Ga, Rh, In, and Tl), $PdBO_2$ (B = Cr, Co, and Rh), and $PtCoO_2$.[21] In general, the techniques involved low temperatures (e.g., metathesis reactions with formation of fused salt byproducts) or oxidizing conditions (e.g., oxidizing flux reactions) or a combination of both (e.g., hydrothermal reactions). The palladium and platinum delafossite-type oxides were generated through metathetical ($PdCoO_2$, $PdCrO_2$, $PdRhO_2$, and $PtCoO_2$), acidic hydrothermal ($PtCoO_2$) reactions, or high-temperature reactions with elevated oxygen partial pressures ($PdCoO_2$ and $PtCoO_2$). An in situ redox reaction between a mixture of the pure metal and metal salt reactants (e.g., Pd and $PdCl_2$) was employed to generate the monovalent palladium and platinum. Copper and silver delafossite-type oxides were synthesized under basic hydrothermal conditions from a combination of the monovalent A-site and trivalent B-site reactants. Similar to the conditions employed by Croft, Tombs, and England,[23] the hydrothermal syntheses were carried out at slightly higher temperatures (500−700 °C) and pressures (3000 atm) in thin-walled platinum or gold tubes.[21]

The hydrothermal synthesis of crystalline copper delafossite-type oxides demonstrated that closed system syntheses are not limited to the syntheses of noble metal delafossite-type oxides only. Indeed, when compared to conventional high temperature solid state chemical reactions, these closed system syntheses offer a relatively low temperature approach to the production of all four A-site cation delafossite-type oxides. Subsequently, numerous syntheses of delafossite-type oxides have relied on these metathetical (cation-exchange),[24−28] oxidizing flux,[29] and hydrothermal[30] reactions. Shannon, Rogers, and Prewitt noted various limitations, however, to each of the three closed system techniques. First, in the case of silver delafossite-type oxides the metathesis reactions often lead to formation of highly stable metal halides (e.g., AgCl) with little to no delafossite-type oxide obtained. An oxidizing flux reaction, where the flux is removed with a postsynthetic leaching step, results in higher yields of the delafossite phase but the presence of a second phase (e.g., Ag_2O), leached out by nitric acid after the reaction, is also reported for some compositions. For copper and silver delafossite-type oxides high temperature and pressure hydrothermal reactions under alkaline conditions is the most effective synthetic route, especially with respect to reducing the amount of undesired phases in the product. Following the pioneering work of Shannon, Rogers, and Prewitt,[21] we pursued the strategy of lowering the temperature (<210 °C) and pressure (<20 atm) required to synthesize copper and silver delafossite-type oxides. In reviewing these efforts, we describe the effect metal oxide solubility and aqueous cation speciation, concepts historically rooted in geochemistry and corrosion science, can have on preparative inorganic chemistry.

2. Hydrothermal Synthesis

While the field of hydrothermal chemistry has been reviewed,[31−33] it is beneficial to consider briefly the main principles that underlie the concepts of a hydrothermal reaction. Hydrothermal syntheses involve chemical reactions in water above ambient temperature and pressure in a sealed or closed system and are a special type of chemical transport reaction that relies on liquid-phase transport of reactants to nucleate formation of the desired product. Under autogenous conditions, water functions both as a pressure-transmitting medium and as a solvent. In a sealed vessel, the vapor pressure of water increases as the temperature is raised above its normal boiling temperature, but below its critical temperature. The selected reaction temperature and the degree of fill, or the percent of the reaction vessel free volume that is filled with water at room temperature, determine the prevailing experimental pressure.[34] When water is used as a solvent, the dielectric constant and viscosity are also important. These decrease with rising temperature and increase with rising pressure, the temperature effect predominating.[35,36] Owing to the changes in the dielectric constant and viscosity of water, the increased temperature within a hydrothermal medium has a significant effect on the speciation, solubility, and transport of solids. Therefore, the hydration of solids and the hydrolysis and speciation of aqueous cations at elevated temperatures, important concepts in this chemistry, are reviewed, briefly, in the following sections.

2.1. Metal Oxide Hydration and Aqueous Cation Speciation. As a solvent, water typically complexes soluble reactants and chemical transport of these complexes at elevated temperatures leads to crystallite growth. The behavior of solid metal oxides and their corresponding cations in aqueous solutions is complex, but nonetheless important to understand metal speciation under a wide range of aqueous conditions, including hydrothermal conditions.[37−39] Although at room temperature solid metal oxides are often insoluble, the hydration of these solid metal oxides can occur. A classic example is the alumina system with hydration reactions relating solid corundum (α-Al_2O_3), boehmite (γ-AlOOH), and gibbsite (γ-$Al(OH)_3$), Scheme 1.[40]

In general, an increase in temperature and/or decrease in pressure thermodynamically favors the less hydrated solid oxide phases.[39] Water can persist, however, in hydrous

Scheme 1. Alumina System with Hydration Reactions Relating Al_2O_3, AlOOH, and $Al(OH)_3$

$$Al_2O_3(s) + H_2O(l) \rightleftharpoons 2\ AlOOH(s)$$

$$AlOOH(s) + H_2O(l) \rightleftharpoons Al(OH)_3(s)$$

$$Al_2O_3(s) + 3\ H_2O(l) \rightleftharpoons 2\ Al(OH)_3(s)$$

Scheme 2. At Progressively Higher pH, the Solubility of α-GaOOH Is Governed by Stepwise Hydrolysis Species

$$GaOOH(s) + 3\ H^+(aq) + 4\ H_2O(l) \rightleftharpoons Ga(H_2O)_6^{3+}(aq)$$

$$GaOOH(s) + 2\ H^+(aq) + 4\ H_2O(l) \rightleftharpoons Ga(OH)(H_2O)_5^{2+}(aq)$$

$$GaOOH(s) + H^+(aq) + 4\ H_2O(l) \rightleftharpoons Ga(OH)_2(H_2O)_4^{+}(aq)$$

$$GaOOH(s) + 4\ H_2O(l) \rightleftharpoons Ga(OH)_3(H_2O)_3(aq)$$

$$GaOOH(s) + 2\ H_2O(l) \rightleftharpoons Ga(OH)_4^-(aq) + H^+(aq)$$

structures at high temperature whether the hydrated phase is stable or not relative to the pure oxide or a less hydrated phase. Conversely, metal oxides can often persist in aqueous solutions at low temperature and therefore not undergo transition to the thermodynamically stable oxide hydroxide or trihydroxide. In the latter instance, a hydrated layer on the metal oxide surface prevents further nucleation of the unstable phase (e.g., corundum is rapidly covered with a series of amorphous AlOOH and $Al(OH)_3$ surface layers upon exposure to low pressure water vapor at room temperature).[38] The formation of these surface layers can passivate the oxide and therefore influence its solubility. Thus, it is important to establish which phase of a given oxide phase is controlling the solubility of the metal of interest in hydrothermal solutions. Interconversions between solid phases, their surface layers, and the rate at which they occur are controlled by the pressure, temperature, pH, and aging time of the solid in the aqueous solution. In most cases, the phase which controls the solubility can only be inferred from observed solubilities under well-defined conditions.[39] Metal oxide−water systems, such as aluminum and gallium, are well-characterized. For other metal oxides, even for important metal oxides such as iron and chromium, the solubility-controlling phase can be difficult to ascertain.

In addition to these hydrated solid metal oxide phases, there are also various aqueous metal species in solution. For example, α-GaOOH when placed in strong acid solutions forms the octahedral $Ga(H_2O)_6^{3+}{}_{(aq)}$ aquo metal complex. At progressively higher pH values the solubility of α-GaOOH is governed by stepwise hydrolysis reactions involving the loss of a proton from an associated water to form a hydroxide group, Scheme 2.[41] During the sequence of successive hydrolysis steps, the overall charge of the metal complex is correspondingly reduced, and the resulting ions differ in their chemical properties such as solubility, surface adsorption, and reactivity.[38] Thus, with increasing pH, $Ga(H_2O)_6^{3+}$ proceeds through the series of complexes shown in Scheme 2 until $Ga(OH)_4^-$ dominates in strongly alkaline solutions, and indeed a lowered coordination number may often be present in anionic hydroxide complexes. Specifically, in basic solutions the tetrahedral configuration is favored for the hydroxide complexes of most trivalent cations (e.g., $Ga(OH)_4^-$).[39] Furthermore, at moderate to high cation concentrations, polynuclear hydrolysis species can also be generated in solution.

Scheme 3. In Terms of Chemical Behavior, Oxides Are Classified as Basic, Acidic, or Amphoteric[a]

(a) Basic Oxide $\quad CaO(s) + 2\ H^+(aq) \longrightarrow Ca^{2+}(aq) + H_2O(l)$

(b) Acidic Oxide $\quad Sb_2O_5(s) + 2\ OH^-(aq) + 5\ H_2O(l) \longrightarrow 2\ Sb(OH)_6^-(aq)$

(c) Amphoteric Oxide $\quad Al_2O_3(s) + 6\ H^+(aq) \longrightarrow 2\ Al^{3+}(aq) + 3\ H_2O(l)$

$\quad Al_2O_3(s) + 2\ OH^-(aq) + 3\ H_2O \longrightarrow 2\ Al(OH)_4^-(aq)$

[a] (a) Basic oxides dissolve in acid, (b) acidic oxides dissolve in bases, and (c) amphoteric oxides dissolve in both.[43]

In 1976, Baes and Mesmer provided a comprehensive and quantitative review on the hydrolysis, speciation, and solubility of metal cations as related to their size, charge, and acid−base character.[37] Since then, many new techniques[38] have been developed to better characterize the behavior of metal cation species in aqueous solution that build upon the basic principles of metal cation speciation and hydrolysis, and how they relate to solubility, outlined by Baes and Mesmer. Metal cation speciation and the chemical behavior of these species in aqueous solution are temperature, metal concentration, pH, and Eh (the reduction−oxidation potential) dependent. With metal oxides, which often are not soluble at room temperature, dissolution rates and therefore solubility increase with temperature. With pH, in general, metal oxide solubility increases with strong acid and/or base concentration; however, the rate of dissolution, often different in acids versus bases, varies for each metal oxide. Thus, the cationic metal species concentration depends sensitively on the solution pH, reflecting the Brønsted reactions with the waters of hydration. Depending on the particular metal oxide, these bound aquo ligands act as proton donors, protons acceptors, or both (amphoterism) as a function of the solution pH,[37] Scheme 2. The solubility of various metal oxides as a function of pH has been described traditionally using the concept of acid−base character, which is briefly reviewed below.

2.2. Metal Oxide Acid−Base Character. In terms of qualitative chemical behavior at various pH, it is convenient to classify oxides according to their acid or base character in the aqueous system. Traditionally, metal oxides can be classified as having acidic, basic, or amphoteric character, based on the electronegativity of the cation.[42,43] Basic oxides such as group 1 and group 2 oxides are characterized by strong ionic bonding and generally dissolve in acids. Composed of nonmetals and less electropositive metals, acidic oxides possess more covalent character and dissolve in alkaline solutions. For transition metals, an increase in charge of the cation leads to a more acidic oxide (e.g., MnO is basic, Mn_2O_7 is acidic). The tendency of an oxide system to dissolve in both acids and bases defines an amphoteric oxide, Scheme 3.

While the classification of metal oxides as acids, bases, or both (ampholytes) is a convenient way to represent the aqueous behavior of an oxide and holds historical importance, it can be difficult to discern the boundary between amphoteric and acidic/basic oxides. Indeed, there is reason to suppose that metal oxides possess some degree of both acidic and basic character (amphoterism), but for the majority of metal

oxides the dominant acidic or basic character overshadows the opposing character. For example, there are metal oxides whose basic properties dominate and therefore form insoluble metal hydroxides in nonacidic, aqueous solutions; however, in very strong bases these metal hydroxides will dissolve slightly. This suggests that these metal oxides can also exhibit some acidic and therefore amphoteric character in strong bases. To resolve whether a metal oxide is amphoteric or not, various methods have been used to assess "borderline" metal oxides.[44−46] With respect to our hydrothermal syntheses in basic solutions, one particularly relevant assessment was a study by Lewis and Anthony that defined an amphoteric oxide as a metal oxide that dissolves in aqueous, alkaline solutions to significantly absorb in the 200−400 nm UV−visible region; otherwise, they were considered basic.[47] The absorption has been assigned to the oxygen $\pi-\pi^*$ electronic transition of the complex, a dissolved metal hydroxide species, $[(M^{x+})_y(OH)_z]^{xy-z}{}_{(aq)}$. In our study, Lewis and Anthony's correlation between solubility and amphoteric character provides a metric to assess whether a metal oxide would dissolve and therefore react. Indeed, metal oxides defined as amphoteric generate delafossite-type oxides; basic oxides do not react, but generate, as expected, stable metal hydroxides. Lewis and Anthony studied 26 different elements. Six of the trivalent B-site cations utilized in the present study were investigated (Al^{3+}, Cr^{3+}, Fe^{3+}, Ga^{3+}, In^{3+}, and Tl^{3+}) and seven were not (Sc^{3+}, Mn^{3+}, Co^{3+}, Ni^{3+}, Y^{3+}, Rh^{3+}, and La^{3+}). In addition, neither of the monovalent A-site cations (Cu^{+}, Ag^{+}) utilized here were studied by Lewis and Anthony. For the metal oxides not investigated by Lewis and Anthony, a combination of published alkaline solubility data, speciation diagrams, and Eh−pH diagrams, at both ambient and elevated temperatures, were consulted to determine their solubility.

2.3. Speciation and Eh−pH (Pourbaix) Diagrams. Speciation and Eh−pH diagrams are commonly used in the areas of geochemistry and corrosion science where the transport, solubility, speciation, and mineralization of metal oxides in hydrothermal systems have been studied extensively. Since aqueous solubility and cation speciation are dependent on pH, the pH controls not only which solid phase is formed but also whether one is formed at all. Speciation diagrams, therefore, chart the different hydrolysis species of a metal cation and their abundance as determined by the solution pH. Furthermore, reactions in which elements adopt various oxidation states are also dependent on the oxidation potential of the solution in addition to the pH value. It is important, therefore, to consider the charge on a cation since the solubility, stability, and ligand lability of a metal cation can be altered through changes in oxidation state. Eh−pH diagrams are a useful way to summarize redox properties and chemical speciation for reactions in which metals capable of existing in different oxidation states participate. In Eh−pH diagrams the reaction equilibria and dominant metal species are plotted in relation to the redox potential and pH, and thus can be seen as a map in the chemical space that summarizes thermodynamic possibilities. Eh−pH diagrams originally acquired significance in applications to corrosion problems as exemplified by the research of Marcel Pourbaix; thus, in the literature they are often called Pourbaix diagrams.[48,49] The construction of such diagrams is discussed in numerous literature sources.[50,51]

While most speciation and Eh−pH diagrams are constructed from experimental information collected under ambient conditions, another important variable to consider in constructing these diagrams is temperature because of the effect on the solvent and the metal cation. Specifically, there is considerable scientific and practical interest in the application of Eh−pH diagrams at higher temperatures and pressures toward preparative hydrothermal chemistry. The construction of elevated temperature Eh−pH diagrams, however, requires the necessary experimental data (e.g., Gibbs free energy, standard molar entropy, and specific heat capacity) under hydrothermal conditions.[52] Therefore, with the exception of the common industrial (i.e., first-row transition) and geological (i.e., main-group) element−H_2O systems, the existence of high temperature Eh−pH diagrams for other element−H_2O systems is incomplete. To overcome this, numerous high temperature element−H_2O systems have been extrapolated from room temperature data.[31] Although limited by the uncertainty of extrapolated data above 150 °C,[52] calculated Eh−pH diagrams can aid experimental formulations by illustrating the trends in speciation as the temperature increases.[53]

Thus, we enlisted high temperature solubility data and Eh−pH diagrams to aid and understand the synthesis of both copper and silver-delafossite-type oxides. For several metal oxides (e.g., Sc_2O_3, Rh_2O_3, and Tl_2O_3) and oxidation states (e.g., CoOOH and NiOOH) without high temperature data, ambient temperature solubility data, if available, were used and compared to metal oxides for which high temperature data were known. A more comprehensive review of the application of Eh−pH diagrams to preparative hydrothermal chemistry, including examples of Eh−pH diagrams, has been prepared by Rabenau.[31]

3. Experimental Section

3.1. Teflon Pouch Method. Prior to the 1980s, most hydrothermal syntheses utilized supercritical temperatures to generate single crystals of inorganic solids.[31] Owing to the corrosive nature of the reaction solution and the possibility of contamination of the product with material from the pressure vessel walls, it was often necessary to fabricate the pressure vessel from carefully selected corrosion-resisting and thermostable alloys. The advent of Teflon-lined pressure vessels reduced both the cost and materials consideration of hydrothermal reactions. Since Teflon tends to be porous, isostatically treated pore-free poly(tetrafluoroethylene) (PTFE) Teflon is used. Pressure vessels fabricated with PTFE Teflon are functional within a limited temperature (<275 °C) and pressure range (<340 atm). Thus, the vast majority of reactions are performed in the subcritical regime at moderate temperatures (<250 °C) and autogenous pressures.

With standard PTFE Teflon-lined stainless steel pressure vessels, one experiment per vessel can be performed, and exploratory synthesis would require numerous vessels and consume a significant amount of time. To overcome this obstacle, combinatorial exploration can be employed to rapidly gain understanding of a chemical reaction under hydrothermal conditions.[54−56] Recently, a technique was reported whereby multiple FEP Teflon pouches are employed

as individual reaction vessels placed within a single pressure vessel of significantly larger size.[57,58] The sealed pouches are semipermeable to water and air under reaction conditions, but not to the solid materials. The operating temperature of FEP films, and thus the reaction temperature, is limited to a maximum of 220 °C. The advantage of the "Teflon pouch" technique is that it allows subtle variations in reactant and mineralizer concentrations with a series of analogous experiments to be performed in a single pressure vessel, while maintaining other reaction variables constant such as temperature, solvent concentration, and time.

3.2. Role of NaOH Mineralizer. If elevated temperatures alone are insufficient to dissolve the solid reagents, then a mineralizer can be added, whose ions form complexes with the solids and render them more soluble. These solubilizing reagents include acids, bases, and alkali salts. Traditionally, bases such as NaOH and KOH have been used as mineralizers in the hydrothermal preparation of delafossite-type oxides at higher temperatures and pressures.[21,23] For example, the original syntheses of $CuFeO_2$[59] and $AgFeO_2$[22] incorporated a boiling NaOH solution. Both the conversion and reaction rate increased with NaOH concentration, consistent with the solubility of the constituent metal oxides and oxide hydroxides increasing at higher pH. Furthermore, while acidic and basic mineralizers increase the solubility of metal oxides by altering the pH, it is also important to consider the effects of the corresponding ions added in addition to protons or hydroxide ions. Complexation of metals by ligands other than water and hydroxide can have profound effects on the total solubility of metal oxides, influencing the stability of dissolved cations at high temperatures.[60] Specifically, in the case of strong base mineralizers, there exists a general disagreement on the stability of ion pairs of alkali metal cations (i.e., Na^+, K^+) and metal complexes (i.e. $Al(OH)_4^-$) in basic media.[61] Thus, while the role of the alkali metal cations is unclear, the primary role of the NaOH mineralizer in the synthesis of delafossite-type oxides is to increase the solubility of the metal complexes by increasing the hydroxide concentration.

In addition to functioning as a mineralizer, NaOH controls the amount of water that enters the FEP Teflon pouch during the reaction. NaOH is known to deliquesce, to become liquid, and to dissolve through absorption of moisture from the air. Consequently, it must be weighed quickly and efficiently to ensure that this does not happen. Before use, NaOH pellets are ground into a fine powder and heated in a vacuum oven at approximately 125 °C to remove a large fraction of the water, thereby fusing the material. To weigh accurately the NaOH, the mass must be broken into small particles. Once the starting materials and the fused NaOH are weighed properly and the pouch is sealed, there are only solid materials inside. Water enters the FEP Teflon pouch once it becomes permeable above ~150 °C. The total amount of water entering each Teflon FEP pouch at elevated temperatures is a function of both the autogenous pressure generated and the amount of fused NaOH in the pouch, with the latter predominating. As expected, with respect to pressure, an increased temperature or water backfill increases the amount of water in each of the pouches. If NaOH mineralizer is not placed in the pouch, however, water will not enter the pouch regardless of the reaction temperature because the primary driving force for the passage of water into the pouch is the presence of fused NaOH and its solvation.

The amount of fused NaOH added to the Teflon pouch prior to the reaction allows for control over the final hydroxide concentration and therefore the delafossite-type oxide product yield. The final hydroxide concentration within the pouch is calculated knowing both the amount of sodium hydroxide added to the sealed pouch and the mass change of the pouch. The latter is attributed to the amount of water permeating the FEP Teflon pouch once it becomes

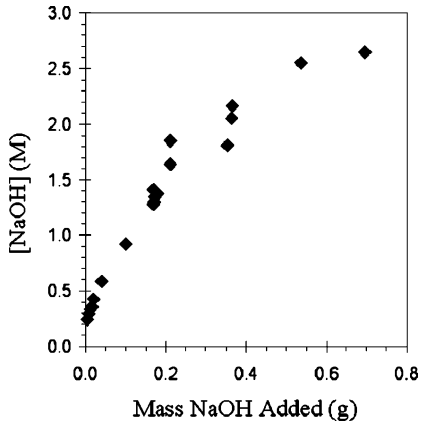

Figure 2. A graph showing how the hydroxide concentration inside the FEP Teflon pouch increases, although not linearly, with the amount of dry, fused NaOH added.

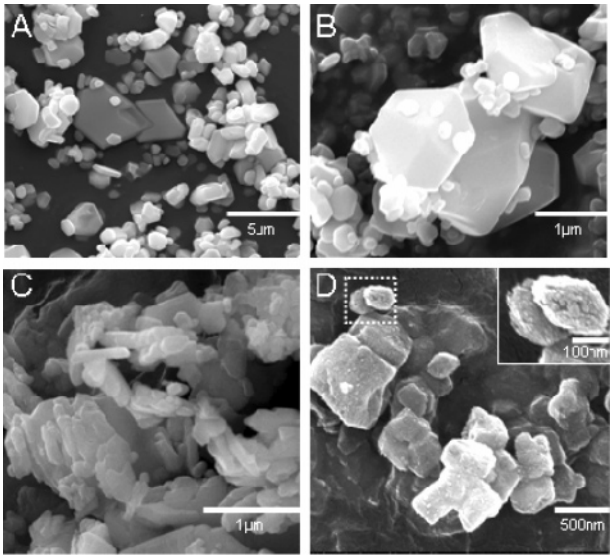

Figure 3. SEM images are shown for (a) a mixture of $AgFeO_2$ crystallites ranging in size from a few tenths of a micrometer up to ~5 μm, (b) a close-up view of some micrometer-sized hexagonal plates of $AgNiO_2$, (c) sub-micrometer crystallites of $AgScO_2$, and (d) 3R-$CuCrO_2$ crystallites, where we observe PXD peak broadening, ranging in size from 100 to 500 nm, with the inset showing a close-up of some of the smallest 3R-$CuCrO_2$ crystallites.

porous at elevated temperatures. Measuring the pH of the backfill (i.e., distilled water outside of the pouch) after the reaction to be neutral (pH = 7) confirms that there is no net diffusion of OH^- ions from the pouches. Although not a linear relationship, an increased amount of fused sodium hydroxide results in a greater final hydroxide concentration, Figure 2. Thus, the synthesis of each delafossite-type oxide was attempted with varying amounts of fused NaOH in individual Teflon pouches. The hydroxide concentrations were then correlated with the mass yield of the products, as determined by PXD, to establish the optimum range of hydroxide concentrations where each delafossite-type oxide formed and where they formed with the maximum yield.

Acidic mineralizers such as HNO_3, HCl, and H_2SO_4 could not be used because of their propensity either to incorporate anions into the reaction or to react immediately with the starting materials to form stable precipitates which did not react during the synthesis. Specifically, these acids promoted the disproportionation of Cu_2O to copper metal and aqueous Cu^{2+} species, the latter stabilized by the corresponding nitrates, chlorides, and sulfates.[62] For the same reason metal nitrates and halides, common hydrothermal precursors, were avoided. From the standpoint of aqueous Cu^+ chemistry, it

Scheme 4. Reaction Scheme between the Monovalent A-Site Cation Metal Oxide and the B-Site Cation[a]

(a) $\frac{1}{2}\ A_2O(s) + \frac{1}{2}\ B_2O_3(s) \xrightarrow{NaOH} ABO_2(s)$

(b) $\frac{1}{2}\ A_2O(s) + BOOH(s) \xrightarrow{NaOH} ABO_2(s) + \frac{1}{2}\ H_2O(l)$

(c) $\frac{1}{2}\ A_2O(s) + B(OH)_3(s) \xrightarrow{NaOH} ABO_2(s) + \frac{3}{2}\ H_2O(l)$

[a] (a) Sesquioxide, (b) oxide hydroxide, or (c) trihydroxide to form delafossite-type oxides.

also should be noted that the Cu^+ ion generated in acidic solutions, with some coordinated water, has a different solubility and chemical reactivity than $Cu(OH)_2^-$ produced in alkaline solutions. As a result, reactions involving common acidic mineralizers do not form delafossite-type oxides. In addition, organic acids such as acetic or oxalic acidic could not be used since they decompose to carbon dioxide under hydrothermal conditions, which then reacts with water and most soluble trivalent B-site cations to generate stable metal carbonates.

3.3. Synthetic Procedure. All reactions were performed with commercially available Cu_2O (99.9% metals basis, Alfa Aesar) or Ag_2O (99.99% metals basis, Alfa Aesar) and the appropriate (described later) sesquioxides, oxide hydroxides, or trihydroxides. Copper- and silver-based delafossite-type oxides were synthesized by adding an equimolar amount of both the A_2O (A = Cu and Ag) and B_2O_3 (B = Al, Sc, Mn, Fe, Ga, In, and Tl), BOOH (B = Al, Fe, Co, and Ni) or $B(OH)_3$ (B = Al, Sc, Cr, and Rh) totaling 0.80 g, with fused NaOH into a fluoro(ethylene-propylene) (FEP) Teflon pouch according to Scheme 4**,** and sealed. Iron,[63] cobalt,[64] and nickel[65] oxide hydroxides and aluminum,[40] chromium,[66] and scandium[67] hydroxides were prepared as described in the literature sources (see Supporting Information). All metal oxide hydroxides and hydroxides were dried thoroughly to ensure accurate weighing of mass amounts and to prevent prehydration of the sealed reaction mixtures.

For any individual preparation, multiple pouches were placed each in a 125-mL PTFE Teflon-lined pressure vessel (Parr Instruments), which was then back-filled with 50 mL of distilled water. The pressure vessel was then sealed and heated to 150 °C, followed by a controlled incremental increase over 5 h to the desired reaction temperature, from 175 to 210 °C depending on the delafossite-type oxide. The maximum temperature was held constant for 60 h with subsequent cooling to room temperature at 6 °C/h. After the latter step, the pouch was opened and polycrystalline delafossite-type oxide products were recovered by filtration, followed by a deionized water rinse to remove any NaOH. All solids collected were then dried at 80 °C for at least 12 h in a drying oven.

3.4. Characterization. Syntheses to prepare copper- and silver-based delafossite oxides, $A^+B^{3+}O_2$ where B^{3+} = Al, Sc, Ti, V, Cr, Fe, Mn, Co, Ni, Ga, Y, Rh, In, La, and Tl, result in single-phase or multiphase samples as determined by powder X-ray diffraction (PXD). PXD data for the samples, to confirm phase formation and extent of purity, were collected every 0.05° for $10° < 2\theta < 80°$ on a Rigaku XDS 2000 diffractometer with Ni-filtered Cu Kα radiation (λ = 1.5418 Å). Polycrystalline samples of $CuBO_2$ (B = Al, Sc, Cr, Mn, Fe, Co, Ga, and Rh) and of $AgBO_2$ (B = Al, Sc, Fe, Co, Ni, Ga, Rh, In, and Tl) form under hydrothermal conditions in basic solutions. Tables 1 and 2 summarize which combinations of A- and B-site metal oxides form a single phase according to PXD. The PXD patterns of pure phase delafossite-type oxide samples can be indexed as either the 3R ($R\bar{3}m$) or 2H ($P6_3/mmc$) delafossite polytype, or a mixture of both. Where available, the PXD patterns were matched to their respective JCPDS files using the Jade software suite,[68] Table 3. Delafossite-type oxides not having a JCPDS file were matched to calculated PXD patterns generated from published crystallographic data by the PowderCell software suite,[69] Table 4.

A significant intensity enhancement for the (00*l*) reflections in the patterns suggests microstructures with a preferred *c*-axis orientation of the grains, which is typical of the majority of the delafossite-type oxides prepared by this method. Electron microscopy studies of delafossite-type oxides were carried out using an Hitachi S-4500 scanning electron microscope (SEM). The SEM

Table 1. Reaction Conditions and Product for the Attempted Synthesis of Certain Copper Delafossite-Type Compounds

reactants	NaOH (M)	temp (°C)	time (h)	product(s)[a]
$Cu_2O + CuO + Al + Al_2O_3$	0.9	210	60	$CuAlO_2$ (3R)
$Cu_2O + 2Sc(OH)_3$	2.5	210	60	$CuScO_2$ (2H, 3R)
$Cu_2O + Ti_2O_3$	1.0	210	60	Cu, TiO_2
$Cu_2O + V_2O_3$	1.0	210	60	Cu, V_2O_5
$Cu_2O + 2Cr(OH)_3$	2.5	210	60	$CuCrO_2$ (3R)
$Cu_2O + 2FeOOH$	1.5	210	60	$CuFeO_2$ (2H, 3R)
$Cu_2O + Mn_2O_3$	1.5	210	60	$CuMnO_2$ (*C*2/*m*)
$Cu_2O + 2CoOOH$	2.0	210	60	$CuCoO_2$ (3R), Co_3O_4
$Cu_2O + 2NiOOH$	2.0	210	60	CuO, NiO
$Cu_2O + Ga_2O_3$	0.5	210	48	$CuGaO_2$ (3R)
$Cu_2O + Y_2O_3$	2.5	210	60	Cu_2O, $Y(OH)_3$
$Cu_2O + 2Rh(OH)_3$	2.5	210	60	$CuRhO_2$ (3R)
$Cu_2O + In_2O_3$	2.5	210	60	Cu_2O, $In(OH)_3$
$Cu_2O + La_2O_3$	2.5	210	60	Cu_2O, $La(OH)_3$
$Cu_2O + Eu_2O_3$	2.5	210	60	Cu_2O, $Eu(OH)_3$
$Cu_2O + Tl_2O_3$	2.5	210	60	Cu_2O, Tl_2O_3

[a] As determined by PXD.

Table 2. Reaction Conditions and Product for the Attempted Synthesis of Certain Silver Delafossite-Type Compounds

reactants	NaOH (M)	temp (°C)	time (h)	product(s)[a]
$Ag_2O + Al_2O_3$	0.9	210	60	$AgAlO_2$ (3R)
$Ag_2O + 2Sc(OH)_3$	2.5	210	60	$AgScO_2$ (2H, 3R)
$Ag_2O + Ti_2O_3$	1.0	210	60	Ag, TiO_2
$Ag_2O + V_2O_3$	1.0	210	60	Ag, V_2O_5
$Ag_2O + 2Cr(OH)_3$	2.5	210	60	Ag, CrO_4^{2-}(aq)[b]
$Ag_2O + Mn_2O_3$	1.5	210	60	Ag, $Na_xMnO_2{\cdot}yH_2O$
$Ag_2O + 2FeOOH$	1.5	180	60	$AgFeO_2$ (2H, 3R)
$Ag_2O + 2CoOOH$	2.0	210	60	$AgCoO_2$ (3R), Co_3O_4
$Ag_2O + 2NiOOH$	2.0	210	60	$AgNiO_2$ (2H, 3R)
$Ag_2O + Ga_2O_3$	0.2	180	48	$AgGaO_2$ (3R)
$Ag_2O + Y_2O_3$	2.5	210	60	Ag_2O, $Y(OH)_3$
$Ag_2O + 2Rh(OH)_3$	2.5	210	60	$AgRhO_2$ (3R)
$Ag_2O + In_2O_3$	1.0	180	48	$AgInO_2$ (3R)
$Ag_2O + La_2O_3$	2.5	210	60	Ag_2O, $La(OH)_3$
$Ag_2O + Eu_2O_3$	2.5	210	60	Ag_2O, $Eu(OH)_3$
$Ag_2O + Tl_2O_3$	2.5	210	60	$AgTlO_2$ (3R), Tl_2O_3, Ag

[a] As determined by PXD. [b] As determined by UV−vis absorption.

Table 3. Delafossite-Type Oxides Matched to Their Respective JCPDS Files in the Jade Software Suite

delafossite-type oxide	JCPDS card number	space group	*a* (Å)	*c* (Å)
$CuAlO_2$	35-1401	$R\bar{3}m$	2.857	16.943
$CuScO_2$	40-1038	$P6_3/mmc$	3.223	11.413
$CuScO_2$	79-0599	$R\bar{3}m$	3.216	17.089
$CuCrO_2$	74-0983	$R\bar{3}m$	2.975	17.096
$CuFeO_2$	79-1546	$P6_3/mmc$	3.035	11.449
$CuFeO_2$	39-0246	$R\bar{3}m$	3.035	17.162
$CuGaO_2$	41-0255	$R\bar{3}m$	2.976	17.158
$AgFeO_2$	25-0765	$P6_3/mmc$	3.039	12.395
$AgFeO_2$	75-2147	$R\bar{3}m$	3.039	18.595
$AgCoO_2$	25-0761	$R\bar{3}m$	2.859	18.26
$AgNiO_2$	49-0666	$R\bar{3}m$	2.939	18.37
$AgInO_2$	21-1077	$R\bar{3}m$	3.277	18.877

Table 4. Delafossite-Type Oxides Matched to Simulated PXD Patterns in the Powdercell Software Suite

delafossite-type oxide	space group	a (Å)[a]	c (Å)[a]	reference
$CuCoO_2$	$R\bar{3}m$	2.8488	16.920	21
$AgAlO_2$	$R\bar{3}m$	2.890	18.27	21
$AgScO_2$	$R\bar{3}m$	3.2112	18.538	21
$AgScO_2$	$P6_3/mmc$[b]	3.211	12.359	21
$AgNiO_2$	$P6_3/mmc$[b]	2.939	12.25	72
$AgGaO_2$	$R\bar{3}m$	2.9889	18.534	21
$AgTlO_2$	$R\bar{3}m$	3.568	18.818	21

[a] The lattice parameters are from the listed literature sources and references therein. [b] Where only the 3R structure is reported in the literature, the unit cell parameters have been converted to the 2H form prior to calculating the simulated PXD pattern.

images in Figure 3 illustrate that the particle sizes for delafossite-type oxide crystallites prepared in this study can range from 100 nm to a few micrometers. In addition, the presence of trace amounts of metallic silver detected by PXD in the silver delafossite-type oxide products is not surprising as it has been evidenced in previous attempts at silver-based delafossite-type oxides.[25,70−74] Our prior TEM studies of samples from several commercial vendors reveal Ag_2O to be the source of the silver impurity.[75]

4. Synthesis of Delafossite-Type Oxides

As summarized by Rabenau,[31] for decades geochemists and mineralogists have used their knowledge of the dominant aqueous species at a given pH, oxidation potential, and temperature to interpret the solubility of reactants in elevated temperature aqueous systems, and to thus provide rationale for mineral formation in hydrothermal environments. In preparative hydrothermal chemistry, therefore, it is also beneficial to understand the solubility of each constituent metal oxide as related to the reaction conditions.

The delafossite-type oxides, owing to the large number of possible B-site cations, enable the study of how the aqueous chemistry of individual elements influences product formation, or lack thereof, in hydrothermal syntheses. Essentially, we seek to exploit the speciation of metal oxides and their associated aqueous complexes to determine why certain delafossite-type oxides form and a few others do not. In this paper, we observe that achieving a minimum solubility ($\sim 10^{-4}$ mol/L) for the reactant oxides at the reaction temperature is a necessary condition for a hydrothermal reaction to occur. Furthermore, we illustrate several key factors that enhance the product mass yield of delafossite-type oxides: (1) increasing the acidic character of the A-, B-site constituent metal oxide or both; (2) elevating the NaOH mineralizer concentration in syntheses that involve B-site constituent metal oxides with more basic character; and (3) choosing the most soluble B-site metal oxide precursor (i.e., metal oxide, oxide hydroxide, or trihydroxide). Our observations and results follow and build on those previously established by Shannon, Rogers, and Prewitt.[21] In the following sections we review solubility data for each A-site and B-site constituent oxide involved in our syntheses and discuss how they relate to the formation, or equally important the lack thereof, of each (see Tables 1 and 2) delafossite-type oxide.

4.1. A-Site Cations. The solubility of monovalent copper and silver oxides plays an essential role in formation of all the delafossite-type oxides. The acidic character of the group 11 oxides increases as one descends the periodic table from copper to gold, and therefore the enhanced acidic character of Ag_2O compared to Cu_2O translates into a higher solubility in bases for Ag^+ ions compared to Cu^+ ions. Furthermore, unlike Cu^+ ions, which can disproportionate, aqueous Ag^+ hydroxide species (i.e., $Ag(OH)_2^-$) are stable at room temperature. As will be demonstrated by multiple examples and comparisons, the increased aqueous solubility of Ag^+ ions compared to Cu^+ ions not only plays an important role in reducing the maximum temperature and time required to form the silver delafossite-type oxide phases but also generates silver delafossite-type oxides that did not form analogous copper delafossite-type oxides with the same B-site cation.

Copper. In aqueous solution at room temperature and ambient pressure, Cu^+ ions disproportionate to Cu^{2+} ions and copper metal.[76,77] At elevated temperatures, however, the stability of aqueous Cu^+ species increases because the decreased water dielectric constant destabilizes the more highly charged Cu^{2+} ion, thereby reducing the driving force for disproportionation.[62] An important feature of the Teflon pouch synthesis, therefore, involves the FEP Teflon pouch remaining impermeable to water until ~150 °C, thereby preventing the aqueous disproportionation of Cu^+ species at lower temperatures. Some quantitative experimental information is available on Cu_2O in basic solutions at elevated temperatures. Above 100 °C at alkaline pH, Cu_2O dissolves to form the stable, soluble $Cu(OH)_2^-$ species.[78−80] Cu^+ ions, although stable, are limited in their solubility in alkaline aqueous media, with an estimated maximum of $[Cu^+] \approx 10^{-4}$ M at 200 °C.

Silver. In contrast to Cu^+ ions, the monovalent oxidation state of Ag^+ is stable in water at room temperature, and the amphoteric character of Ag_2O has been demonstrated.[81−83] In strong bases Ag^+ ions exist primarily in the form of soluble $Ag(OH)_2^-$ species. As the temperature increases, Eh−pH diagrams also demonstrate that the region of stability for $Ag(OH)_2^-$ becomes greater, so it is possible for higher concentrations of $Ag(OH)_2^-$ to be present at a given pH.[84] Ag^+ ions have a significantly higher aqueous alkaline solubility when compared to Cu^+ ions, with a maximum concentration of $[Ag^+] \approx 10^{-2.5}$ mol/L at 200 °C, an impressive 30-fold increase. Another important change in the Eh−pH diagrams with an increase in temperature is that the evolution of oxygen from Ag_2O to form silver metal becomes more favorable. Although closed system syntheses reduce the likelihood of spontaneous Ag_2O decomposition, we notice in combination with particular B-site cations, which can undergo oxidation, that a redox reaction occurs (see section on transition metals).

4.2. B-Site Cations. With regard to the delafossite-type oxides, Shannon, Rogers, and Prewitt proposed that the oxidized state of the noble A-site metal, particularly palladium, platinum, and silver, is "apparently" stabilized by the basicity of the companion B-site cation metal oxide.[21] As alluded to previously and summarized below for each individual metal cation, we demonstrate that the acidity of the B-site metal oxide, oxide hydroxides, and hydroxides

allows them to dissolve in the form of metal hydroxospecies, $[B(OH)_y]^{3-y}{}_{(aq)}$, at elevated temperature and alkaline, aqueous conditions and therefore to undergo reaction. Although the basic character of the majority of the B-site metal oxides is well-known, the acidic character of the B-site metal oxides, which is only revealed in strongly alkaline solutions (>1 M), is important to the formation of delafossite-type oxides. Copper and silver delafossite-type oxide products, therefore, result from a reaction between the soluble A-site and B-site cation metal oxide/hydroxide species. In contrast, the most basic B-site cation metal oxides form the insoluble and unreactive trihydroxides, and no delafossite-type oxide product results. In general, the B-site metal oxides can exist as either oxides (B_2O_3), oxide hydroxides, (BOOH) or trihydroxides ($B(OH)_3$). In this paper, when not referring to a specific form of the metal oxide, for the sake of simplicity, the general term metal oxides is used (e.g., gallium oxides refer to all forms of Ga_2O_3, GaOOH, and $Ga(OH)_3$).

4.2.1. Group 3 Metal Oxides. All the group 3 copper delafossite-type oxides ($CuScO_2$, $CuYO_2$, and $CuLaO_2$) were synthesized previously by high temperature reactions between Cu_2O and the corresponding sesquioxide.[85,86] Prior to our synthesis of both $CuScO_2$ and $AgScO_2$, only $AgScO_2$ had been hydrothermally synthesized by Shannon, Rogers, and Prewitt.[21] The reaction of only scandium oxides among the group 3 metal oxides is not surprising as the group 3 oxides have considerable basic character with the basicity increasing for the heavier elements. Yttrium and lanthanum oxides, therefore, are too basic to be significantly soluble in alkaline solutions and form insoluble hydroxides.

Scandium. Similar to the other group 3 metals yttrium and lanthanum, scandium only exists in the trivalent state in solution and its oxides exhibit strongly basic character; however, unlike the heavier group 3 metals, scandium oxides also exhibit amphoteric character.[37] This is because Sc_2O_3, ScOOH, and $Sc(OH)_3$ possess acidic character, although weak, that when combined with their dominant basic character they can be classified as "weakly amphoteric". The solubility of $Sc(OH)_3$ scales with base concentration and therefore requires considerable aqueous concentrations of hydroxide (>10 M) to be appreciably soluble at ambient temperature, with a maximum of $[Sc^{3+}] = 5 \times 10^{-2}$ mol/L in 11 M sodium hydroxide solution.[87] Above the hydroxide concentration at which Sc^{3+} ions are at their maximum solubility, the formation in strong bases of crystalline alkali metal hydroxoscandates, $Na_3[Sc(OH)_6]\cdot 2H_2O$ and $K_2[Sc(OH)_5(H_2O)]\cdot 3H_2O$, are further indication that soluble hydroxoscandate species, $[Sc(OH)_n]^{3-n}{}_{(aq)}$, predominate in very basic solutions.

In the current study, $Sc(OH)_3$ was reacted with Cu_2O and Ag_2O to generate the analogous delafossite-type oxides. It is not known if the $Sc(OH)_3$ transforms into ScOOH before it undergoes reaction since α-ScOOH is the stable form of solid scandium oxide in hydrothermal systems above ∼150 °C.[67] Regardless, we chose $Sc(OH)_3$ as the reactant because Sc_2O_3 does not react with Cu_2O and is slow to undergo transition via hydration, to the more reactive hydrated phases, ScOOH and/or $Sc(OH)_3$. The optimized sodium hydroxide concentration is 2.0 and 2.5 M for the synthesis of $AgScO_2$ and $CuScO_2$, respectively, where at room temperature scandium has a reported solubility of $[Sc^{3+}] \approx 10^{-4}$ mol/L.[87] Both the $CuScO_2$ and $AgScO_2$ product contain a mixture of the 2H- and 3R-polytypes. While phase-pure $AgScO_2$ results (Figure 4) unreacted ScOOH remains in the $CuScO_2$ product. This result can be attributed to the greater solubility of Ag^+ ions than Cu^+ ions. At lower hydroxide concentrations (<2.0 M) no $CuScO_2$ forms and the $AgScO_2$ reaction also contains unreacted ScOOH. At greater hydroxide concentrations (>2.5 M), there is an increase in the dissolution of the ScOOH reactant; however, the $CuScO_2$ yield does not appreciably increase. Instead, the water in the FEP Teflon pouch turns blue, consistent with the enhanced hydroxide concentration, allowing oxygen inside the pouch to oxidize some fraction of the Cu^+ to Cu^{2+}. A 1.0 h soak in 0.5 M HNO_3 at ambient temperature removes any ScOOH from the product while avoiding significant dissolution of the $CuScO_2$.

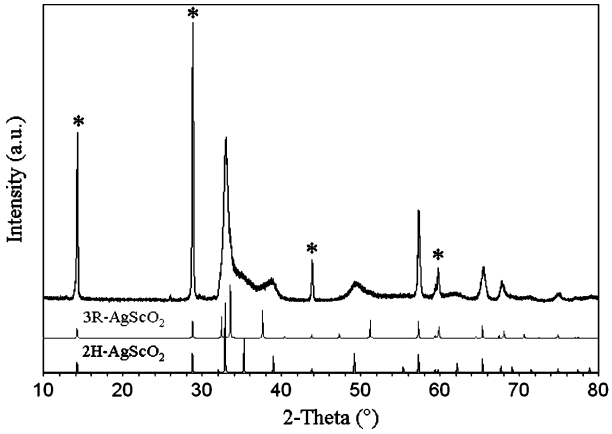

Figure 4. The PXD pattern of the $AgScO_2$ product consists of a mixture of both the 00*l*-ordered (*) 2H- and 3R-polytypes. Calculated positions, both indexed and indicating relative intensities, are shown for 2H-$AgScO_2$ and 3R-$AgScO_2$.[21]

Yttrium and Lanthanum. Yttrium and lanthanum oxides are characterized by predominantly ionic bonding because of the greater differences in electronegativity between the rare-earth cation and oxide anion, resulting in strongly basic character. Consequently, the solubility of yttrium and lanthanum oxide in aqueous alkaline solutions is negligible, even at elevated temperatures, and both yttrium and lanthanum oxide readily hydrolyze to generate the stable, insoluble trihydroxide in water.[88,89] It was not surprising, therefore, that over the range of temperatures (170−210 °C) and hydroxide concentrations (0.2−2.5 M) employed in this study neither Cu_2O nor Ag_2O undergo reaction with Y_2O_3 or La_2O_3 to yield delafossite-type oxides.

4.2.2. Group 13 Metal Oxides. While copper delafossite-type oxides containing the lighter group 13 elements, $CuBO_2$ (B = Al and Ga), have been synthesized by high temperature solid-state reactions,[90] Shannon, Rogers, and Prewitt were the first to synthesize the silver delafossite-type oxides with group 13 B-site cations, $AgBO_2$ (B = Ga, In, and Tl).[21] In the present study, at low temperatures both copper, $CuBO_2$ (B = Al and Ga), and silver, $AgBO_2$ (B = Al, Ga, In, and Tl), delafossite-type oxides were generated, as expected. As will be discussed later, these results are consistent with the general trend of progressively decreasing acidic character

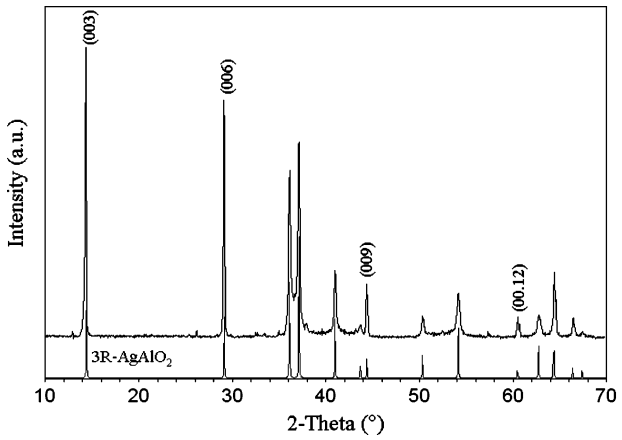

Figure 5. The PXD pattern of the 3R-$AgAlO_2$ product has enhanced 00*l*-ordered reflections consistent with preferred crystalline orientations along the *c*-axis. Calculated positions, both indexed and indicating relative intensities, are shown for 3R-$AgAlO_2$.[21]

and decreasing solubilities of the group 13 oxides in the series aluminum to thallium.

Aluminum. Aluminous phases (e.g., Al_2O_3, AlOOH, and $Al(OH)_3$) are often cited as the classic examples of oxides exhibiting amphoteric character. Solubility data across a broad range of pH and temperatures confirm that aluminous minerals indeed possess amphoteric character.[91−93] The solubility of alumina increases with an increase in temperature and pH, and under alkaline conditions (pH > 9), the aqueous aluminum species $Al(OH)_4^-$ predominates, achieving a measured solubility of $[Al^{3+}] \approx 10^{-1}$ mol/L at 200 °C in 0.5 M hydroxide concentration.[93]

In the present study, phase-pure 3R-$AgAlO_2$ forms in a direct reaction between Ag_2O and AlOOH at a moderate hydroxide concentration (∼1 M) (Figure 5), yet the highest mass yield for a reaction between Cu_2O and AlOOH is ∼60% 3R-$CuAlO_2$. In the synthesis of $CuAlO_2$, the aluminous mineral source, corundum (α-Al_2O_3) vs boehmite (γ-AlOOH), vs gibbsite (γ-$Al(OH)_3$), affects the product mass yield; both boehmite and gibbsite afford an increased product yield compared to corundum. This is clearly a kinetic effect since gibbsite is not stable in aqueous solution above 80 °C, nor is corundum below ∼380 °C; therefore, they both are transformed to boehmite at the reaction temperature of 210 °C. The different aluminous sources react at a different rate, however, because the reaction occurs over a finite time period (60 h), and the phase transformation to boehmite is not spontaneous. Indeed, in the straightforward stoichiometric reaction of Cu_2O with aluminous minerals this was evidenced by the presence of boehmite in the 3R-$CuAlO_2$ product, regardless of the starting material, except in the case of corundum where a mixture of boehmite and corundum is detected. Longer reaction times result in complete dissolution of all alumina reactants, as determined by inductively coupled plasma atomic emission spectroscopy (ICP-AES) of the water inside the pouch. However, a portion of the Cu_2O reactant still remains in the 3R-$CuAlO_2$ product. Our previously reported syntheses of phase-pure 3R-$CuAlO_2$ incorporated a redox reaction between a mixture of Cu_2O/CuO and Al/Al_2O_3 at 210 °C.[94]

Gallium. Below aluminum in the periodic table, gallium oxides exhibit many similar chemical properties, including amphoteric character. Lewis and Anthony[47] reported a significant optical absorption for $Ga(OH)_3$ dissolved in aqueous, basic media, and various metal hydroxogallates, such as $NaGa(OH)_4$, have been isolated under similar conditions.[95] Both of these observations are consistent with the formation of an aqueous soluble gallate ion, $Ga(OH)_4^-$. In fact, gallium oxides are not ideal ampholytes since solubility data collected at both ambient and elevated temperatures demonstrate that their acidic properties are more marked than the basic properties.[96] This agrees well with $Ga(OH)_4^-$ having a solubility on the order of $[Ga^{3+}] \approx 1$ mol/L at 200 °C in 0.5 M hydroxide solution, a magnitude greater than aluminum under similar conditions.[41] As a result of the high solubility of gallate ion, in the present study both 3R-$CuGaO_2$ and 3R-$AgGaO_2$ both form phase pure at 180 °C, the lowest temperature with respect to all delafossite-type oxides synthesized, and at very low hydroxide concentrations (0.2 M) by reaction of Cu_2O or Ag_2O, respectively, with Ga_2O_3.

Indium. In contrast to the lighter group 13 metal oxides Al_2O_3 and Ga_2O_3, In_2O_3 does not dissolve readily in alkaline media at elevated temperatures. While extensively studied, there exists a general disagreement on the exact solubility of indium oxides in basic media.[97] A general consensus can be reached, however, that defines In^{3+} ions as more soluble in acid than in base. Lewis and Anthony support this consensus by defining $In(OH)_3$ as "very slightly amphoteric", owing to the minimal optical absorption of the aqueous species generated from the dissolution of $In(OH)_3$ in 3 M KOH.[47] Polarographic methods,[98] and crystalline hydroxoindates $Na_3[In(OH)_6]\cdot 2H_2O$, $K_3[In(OH)_6]\cdot 2H_2O$, and $Rb_2[In(OH)_5(H_2O)]$[99] isolated from solutions of $In(OH)_3$ in concentrated alkali, provide evidence for the presence of indate ions, $[In(OH)_n]^{3-n}{}_{(aq)}$. Ivanov-Emin et al. report $In(OH)_3$ having a maximum ambient temperature alkaline solubility of $[In^{3+}] \approx 6 \times 10^{-2}$ mol/L at a sodium hydroxide concentration of 11.0 M, a result similar to that of weakly amphoteric scandium.[100] Although both Sc^{3+} and In^{3+} ions have similar maximum concentrations at very high sodium hydroxide concentrations (>10 M), at hydroxide concentrations attainable in the Teflon pouch technique (∼1 M) In^{3+} solubility at room temperature $[In^{3+}] \approx 10^{-5}$ mol/L is a magnitude lower than that of Sc^{3+} ions.[87] As a result, while in the present study phase-pure 3R-$AgInO_2$ readily forms in the reaction of Ag_2O with In_2O_3 at 180 °C, $CuInO_2$ does not form. Instead, the reaction between Cu_2O and In_2O_3 at 210 °C results in the conversion of all the In_2O_3 into $In(OH)_3$. A direct reaction between Cu_2O and $In(OH)_3$ also does not yield $CuInO_2$. The presence of $In(OH)_3$ in the product, In^{3+} ion solubility data, and the lack of $CuInO_2$ product, even at substantial sodium hydroxide concentrations (∼2.5 M), would suggest that $In(OH)_3$ is too basic in character to dissolve at the minimum level required for a hydrothermal reaction with the slightly soluble Cu^+ ions. In contrast, more amphoteric Ag_2O, which has a greater solubility, overcomes this constraint and forms 3R-$AgInO_2$.

Thallium. Following the group trend, Tl_2O_3 and $Tl(OH)_3$ exhibit the most basic character of all the group 13 elements. Their solubility also remains the least studied of the group

13 metal oxides because of their limited use and high toxicity. Ivanov-Emin et al. demonstrated that $Tl(OH)_3$ has the lowest maximum ambient temperature solubility in strong bases (∼12 M) when compared to aluminum, gallium, and indium hydroxides.[101] At hydroxide concentrations more representative of the present experimental conditions (<2.5 M), the room temperature solubility of Tl^{3+} species is slightly lower than that of In^{3+} ions, but still around $[Tl^{3+}] \approx 10^{-5}$ mol/L.

In the current study, the reaction between Tl_2O_3 and Ag_2O at 210 °C and high hydroxide concentration (2.5 M) results in a ∼50% mass yield of 3R-$AgTlO_2$ with Tl_2O_3 and silver metal, from the decomposition of unreacted Ag_2O, comprising the rest of the product. As expected, $CuTlO_2$ does not result in a reaction between Cu_2O and Tl_2O_3 under similar conditions. As before, the formation of $AgTlO_2$, but not $CuTlO_2$, correlates well with the higher solubility of Ag^+ versus Cu^+ ions. Owing to the low solubility of Tl_2O_3 compared to the other group 13 metal oxides and therefore the longer reaction time required to obtain a significant mass yield of $AgTlO_2$, we could not generate phase-pure $AgTlO_2$ because a fraction of the Ag_2O decomposed to silver metal before reacting with poorly soluble Tl_2O_3.

It should be noted that Tl_2O_3 is toxic and should be handled with care. Owing to the toxicity of Tl_2O_3 and the porosity of PTFE Teflon liners at elevated temperatures, the reactions between Cu_2O or Ag_2O and Tl_2O_3 at various hydroxide concentrations (0.5−2.5 M) was limited to one set of reactions, and the Teflon liner was subsequently disposed of, to avoid the hazard of permanent contamination of the reactor. Based on our observations with other sesquioxides, the product yield of $AgTlO_2$ may be improved by utilizing a $Tl(OH)_3$ reagent instead of Tl_2O_3 in the reaction with Ag_2O. These experiments would discern whether the mass yield of $AgTlO_2$ is limited by the transition between Tl_2O_3 and $Tl(OH)_3$ and/or TlOOH, which was not observed, or by the basic character of thallium oxide.

4.2.3. Transition Metals Oxides. The original hydrothermal syntheses of delafossite-type oxides involved the production of the mineral delafossite ($CuFeO_2$) by Emons[59] and its silver analogue ($AgFeO_2$) by Krause.[22] Subsequently, Shannon, Rogers, and Prewitt generated both $CuBO_2$ (B = Cr, Co, and Rh) and $AgBO_2$ (B = Cr, Co, and Rh) delafossite-type oxides at higher temperatures and pressures.[21] In this study, all the aforementioned delafossite-type oxides were generated in addition to $CuCrO_2$, $CuMnO_2$, and $AgNiO_2$.

Chromium. Independent of the trivalent chromium oxide source, at room temperature Cr^{3+}−hydroxo complexes, $[Cr(OH)_n]^{3-n}$, are the dominant aqueous species.[66] The solubility of $Cr(OH)_3$ increases with both proton and to a lesser degree hydroxide concentration,[102] and Cr^{3+} ions in alkaline conditions are stabilized by the formation of the aqueous soluble $Cr(OH)_4^-$ species. Therefore, while the basic character of $Cr(OH)_3$ is slightly more pronounced than its acidic character, it behaves as a "weakly amphoteric" hydroxide. At ambient temperatures and a 2.5 M NaOH concentration used in the present syntheses, $Cr(OH)_4^-$ has an aqueous solubility of $[Cr^{3+}] \approx 10^{-4}$ mol/L.[102] Although to our knowledge the quantitative alkaline, elevated temperature solubility of $Cr(OH)_3$ is unknown, the predominance region for $Cr(OH)_4^-$ in the elevated temperature Pourbaix diagram for chromium−water increases with temperature, indicating that the concentration increases.[103] In contrast, the reported solubility for Cr_2O_3 in alkaline media at 200 °C is negligible (nanomolar).[104] Thus, in the present study we find that while both $Cr(OH)_3$ and CrOOH react with Cu_2O to form phase-pure 3R-$CuCrO_2$ (Figure 6) at 210 °C at a moderate hydroxide concentration (>1.0 M), Cr_2O_3 did not react under similar experimental conditions to form $CuCrO_2$. Based on these observations, the chromium oxide system is found to behave similarly to the aluminous phase series, demonstrating that although in general the various hydrated metal oxides are amphoteric, a slow transition to the more solublereactant phase limits the formation of the delafossite-type oxide product.

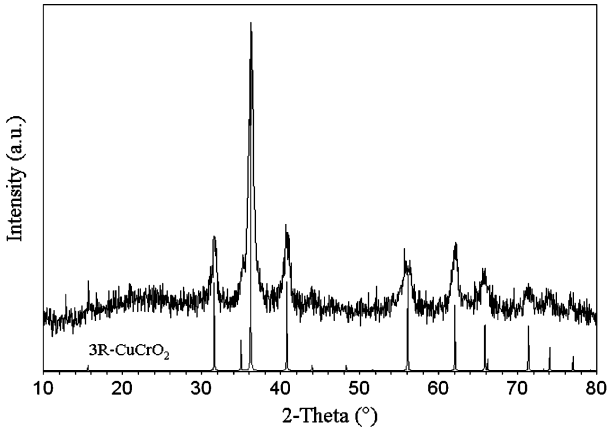

Figure 6. PXD pattern of the small crystallite 3R-$CuCrO_2$ product. Scherrer analysis yields a crystallite size of ∼150 nm, although the SEM image in Figure 2d suggests a crystallite size ranging between 100 and 500 nm. Calculated positions, both indexed and indicating relative intensities, are shown for 3R-$CuCrO_2$ (JCPDS #74-0983).

CrOOH or $Cr(OH)_3$, unlike other amphoteric transition metal oxide hydroxides and hydroxides, does not react with Ag_2O to form $AgCrO_2$, but rather these reactions generate a large amount of silver metal. It has been proposed that, in air at elevated temperatures (but below the decomposition temperature of 300 °C), Ag_2O undergoes slow dissociative evaporation to molecular oxygen and free silver atoms, which immediately condense as metallic silver.[105] While $Ag(OH)_2^-$ remains stable in solution to react and yield silver delafossite-type oxides with other trivalent transition metals (e.g., iron), in the presence of Cr^{3+} ions, which can undergo oxidation to Cr^{6+}, a redox reaction occurs that accelerates the decomposition of Ag_2O to metallic silver and limits the formation of $AgCrO_2$. The yellow color of the FEP pouch water, indicative of the formation of highly soluble CrO_4^{2-} in alkaline solutions, lends further support to the hypothesis that a redox reaction occurred. Similarly, Ti_2O_3, Mn_2O_3, and V_2O_3, other trivalent transition metal oxides, which also readily undergo oxidation, also reduce the Ag_2O to silver metal. Thus, a B-site cation may exhibit amphoteric character, but silver delafossite-type oxide cannot be formed if the soluble trivalent species can easily oxidize.

Manganese. In comparison to chromium and iron, few solubility studies of manganese oxides at elevated temperature have been reported, presumably due to the many

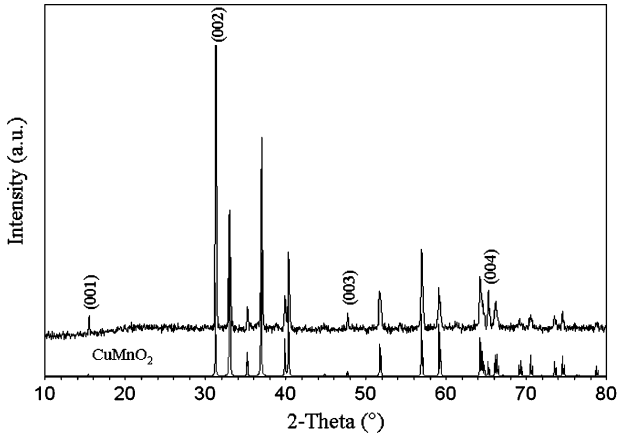

Figure 7. The PXD pattern of the $CuMnO_2$ product has enhanced 00*l*-ordered reflections consistent with preferred crystallite orientations along the *c*-axis. Calculated positions, both indexed and indicating relative intensities, are shown for monoclinic $CuMnO_2$ (JCPDS #50-0860).

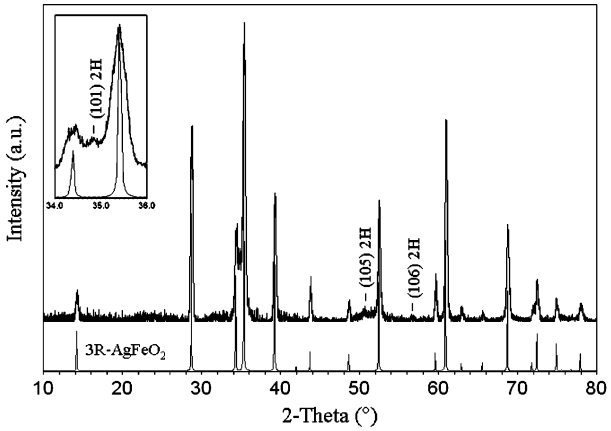

Figure 8. The PXD pattern of the $AgFeO_2$ product consists primarily of the 3R-polytype, with a small amount of admixed 2H-$AgFeO_2$ polytype, with the inset showing the region from $34.0° < 2\theta < 36.0°$ where the most intense peak of 2H-$AgFeO_2$ (JCPDS #25-0765) appears, indexed as (101); other observable 2H-$AgFeO_2$ reflections are indexed as well. Calculated positions, both indexed and indicating relative intensities, are shown for 3R-$AgFeO_2$ (JCPDS #75-2147).

accessible oxidation states (II−VII) and solid oxides prevalent in this system. Divalent manganese hydroxide was classified as "very slightly amphoteric" by Lewis and Anthony; however, no data were collected for trivalent manganese hydroxide.[47] The discrete cluster model, which is treated explicitly with density functional theory on the absolute pK_a of manganese cations in solution surrounded by two hydration shells of water, predicts that waters coordinated to aqueous Mn^{3+} more readily undergo deprotonation to form hydroxo complexes than Fe^{3+} species and therefore are ranked more acidic.[106] Consistent with the expected increase in acidity for an increase in cation oxidation state, the discrete cluster model also predicts that the species containing trivalent ions of iron and manganese are far more acidic than the species incorporating divalent ions. Experimental measurements also support this model since the measured concentration of Mn^{3+} ions at ambient temperature in 3 M NaOH solutions, the lowest hydroxide concentration reported, is $[Mn^{3+}] \approx 10^{-3}$ mol/L, 3 magnitudes larger than the solubility of Fe^{3+} in a similar environment.[107] An increase in the solubility of Mn^{3+} ions with increasing hydroxide concentration correlates with the formation of soluble $[Mn(OH)_n]^{3-n}$ species.

Consistent with the appreciable amphoteric character of Mn_2O_3, in the present study, phase-pure $CuMnO_2$ results from a straightforward reaction between Cu_2O and Mn_2O_3 at 210 °C at a moderate hydroxide concentration (1.5 M). $CuMnO_2$ (also known as the mineral crednerite) does not crystallize in either the 2H- or 3R-delafossite space group.[108] All peak positions correspond to reflections of the monoclinic phase *C*2/*m* (No. 12), with cell constants that match those of JCPDS file #50-0860 ($a = 5.596$ Å, $b = 2.880$ Å, $c = 5.899$ Å, $\beta = 104.02°$; Figure 7). The monoclinic structure of $CuMnO_2$ is closely related to that of delafossite, but the expected Jahn−Teller distortion of Mn^{3+} breaks the 3-fold symmetry along the hexagonal *c*-axis. $CuMnO_2$, therefore, possesses the same stacking of $O-Cu^+-O$ dumbbells and slightly distorted edge-shared $Mn^{3+}O_6$ octahedra. $AgMnO_2$ does not form in the reaction of Ag_2O with Mn_2O_3, but rather Ag_2O is reduced to silver metal and Mn^{3+} is oxidized to form a mixed valent (Mn^{3+}/Mn^{4+}) sodium manganate (Na_x-$MnO_2{\cdot}yH_2O$) identified by PXD. Indeed, it was reported previously that mixed valent sodium manganates (Mn^{3+}/Mn^{4+}) are formed when MnO_2 is subjected to a hydrothermal reaction in the presence of a NaOH mineralizer.[109]

Iron. Owing to its ubiquitous environmental and industrial chemistry, the aqueous corrosion and speciation chemistry of iron has been investigated at both ambient and elevated temperatures. Although ferric oxides do not readily dissolve in basic solutions as do aluminum and gallium oxides, the existence of $Fe(OH)_4^-$ species in basic solutions is reported in various elevated temperature solubility studies of ferric minerals such as $Fe(OH)_3$,[110,111] FeOOH,[112] and Fe_2O_3.[113,114] Goethite (α-FeOOH), the most soluble ferric mineral at 20 °C, has a solubility in alkaline solutions (<2.5 M) on the order of $[Fe^{3+}] \approx 10^{-6}$ mol/L.[112] While the solubility of $Fe(OH)_4^-$ is markedly less than that of other trivalent metal species at room temperature, the solubility of the $Fe(OH)_4^-$ increases at a greater rate with increasing temperature over other trivalent metal species (e.g., $Al(OH)_4^-$ and $Ga(OH)_4^-$). The enhanced dissolution rate for ferric oxides with increasing temperature is attributed to their greater heat capacity, which enhances their entropy and free energy with temperature and therefore their solubility. While the exact value varies slightly between literature sources, the average reported solubility of $Fe(OH)_4^-$ at hydroxide concentrations comparable to these of the present syntheses (∼2.5 M) at 200 °C is $[Fe^{3+}] \approx 10^{-4}-10^{-5}$ mol/L.[113]

In the current study, FeOOH reacts with Cu_2O or Ag_2O at 210 °C and moderate hydroxide concentrations (1.5 M) to form $CuFeO_2$ and $AgFeO_2$, respectively; both products consist of a mixture of 2H- and 3R-polytypes (Figure 8). Lower hydroxide concentrations (<1.5 M) diminish the purity of the $CuFeO_2$, but not of the $AgFeO_2$ product. In addition, employing hematite (α-Fe_2O_3) as the iron oxide reagent also results in $AgFeO_2$ at moderate NaOH concentrations (>1.0 M); however, unreacted Cu_2O and Fe_2O_3 reactants are present in the 3R- and 2H-$CuFeO_2$ products, regardless of the hydroxide concentration (0.5−2.5 M). Based on these observations, FeOOH proved to be a more

reactive iron oxide source in basic solution than α-Fe_2O_3. Our observations on the synthesis of iron delafossites are consistent with previous observations by Feitknecht et al. in the synthesis of $AgFeO_2$ from Ag_2O and FeOOH in boiling NaOH solution;[115] they reported that the reaction rate increases with hydroxide concentration, as does the solubility of the various iron reagents (α, *β*, *γ*, versus *δ*-FeOOH). Furthermore, in addition to planned syntheses,[59] the mineral delafossite ($CuFeO_2$) previously has been evidenced and reported as an unintentional precipitate in boiling water reactors containing both copper oxides and iron oxides at temperatures reaching 290 °C.[116] Although the delafossite product itself was not studied extensively, thermodynamic data collected by the authors argue that under the experimental conditions, where the aqueous stability regions of Cu^+ and Fe^{3+} species overlap, $CuFeO_2$ is more stable than the constituent oxides, Cu_2O and Fe_2O_3.

Cobalt. Compared with more common aqueous Co^{2+} species, little is known about aqueous Co^{3+} species in the cobalt−water system because, in acidic and neutral aqueous solutions, Co^{3+} ions are unstable and decompose at room temperature with the evolution of oxygen and formation of Co^{2+}.[37] Furthermore, most elevated temperature studies of cobalt oxides solubilities do not consider pure Co^{3+} species since the required experimental data are not available.[117] However, when using $Co(OH)_3$ and CoOOH sources under alkaline conditions, Co^{3+} is stable and their solubility increases with increasing hydroxide concentration. Specifically, at a hydroxide concentration of 3.0 M, the room temperature solubility is $[Co^{3+}] \approx 10^{-6}$ mol/L[118,119] a relatively low concentration that is consistent with cobalt oxides exhibiting weak amphoteric character. As with other transition metal cations, however, in elevated temperature Eh−pH diagrams, the concentration of Co^{3+} species is predicted to increase with temperature.[120]

CoOOH was used as the source of Co^{3+} in the present study since we observed neither Co_2O_3 nor Co_3O_4 undergo reaction with the A-cation oxides to form the desired product. Both 3R-$CuCoO_2$ and 3R-$AgCoO_2$ form through a reaction between CoOOH and Cu_2O or Ag_2O, respectively, at 210 °C in strong hydroxide solutions (2.5 M). Both the $CuCoO_2$ and $AgCoO_2$ products are not phase-pure, however, as they contain significant quantities of Co_3O_4 at all hydroxide concentrations (0.2−2.5 M). As expected, the $CuCoO_2$ product contains more Co_3O_4 than does the $AgCoO_2$ product, consistent with the decreased solubility of Cu^+ species versus Ag^+ species. The presence of Co_3O_4 in the product is not surprising since, at elevated temperatures, the Eh−pH diagrams for the cobalt−water system also predict that although Co^{3+} species exist in solution they are metastable and will eventually transform to the mixed valent spinel.

Similar to the original reported syntheses of $AgFeO_2$ by Krause,[22] polycrystalline $CuCoO_2$ and $AgCoO_2$ have been reported for a reaction between the monovalent oxide and CoOOH in boiling NaOH solution.[121] The $CuCoO_2$ and $AgCoO_2$ generated from these reactions were not sufficiently crystalline enough to be indexed by PXD and also contained Co_3O_4. However, the authors did report that the pattern was similar to the known pattern for $CuFeO_2$. Later, another

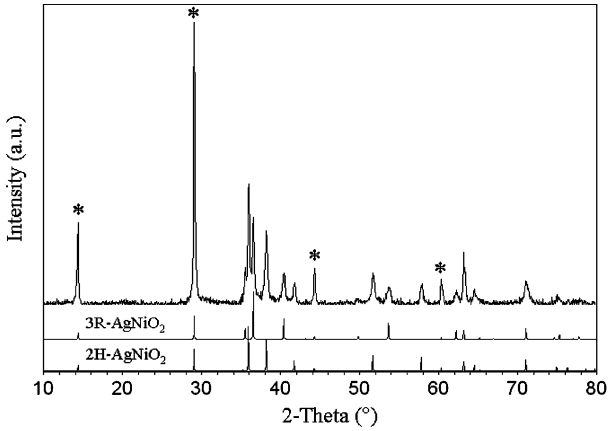

Figure 9. The PXD pattern of the $AgNiO_2$ product consists of a mixture of both the 00*l*-ordered (*) 2H- and 3R-polytypes. Calculated positions, both indexed and indicating relative intensities, are shown for 2H-$AgNiO_2$ and 3R-$AgNiO_2$ (JCPDS #49-0666).

reported reaction between silver metal and CoOOH at 330 °C and at 300 atm in 0.5 M NaOH for 48−72 h generated a $AgCoO_2$ product crystalline enough to be indexed by high-resolution PXD.[122] In the latter reaction, a mixture of both the 2H- and 3R-$AgCoO_2$ phases was observed.

Nickel. Owing to the use of nickel alloys in the high temperature portions of nuclear power plants, the solubility data for NiO and its corrosion products are extensive. However, trivalent nickel oxides were not considered in these studies because Ni^{3+} is unstable at ambient temperature, in acidic and neutral aqueous solutions with respect to the divalent cation. In elevated temperature Eh−pH diagrams for the water−nickel system, however, the stability area of "beta-phase nickel oxide" (trivalent nickel oxides) in alkaline solutions was reported to increase with temperature.[123] Based on this report, the concentration of soluble Ni^{3+} species should increase with increasing temperature, although the authors comment that the calculated temperature dependence of the stability areas of the "higher oxides of nickel" should be viewed with a certain degree of caution until further experimental evidence is available. Prior to the present synthesis, however, the synthesis of $AgNiO_2$ had been reported via an aqueous reaction between NiOOH and Ag_2O in a strong KOH solution at room temperature.[15] The PXD for this room temperature $AgNiO_2$ was characterized by very broad diffraction peaks, which were indexed by the author to the known 3R-delafossite $AgCoO_2$ phase, invoking the similar sizes of the Co^{3+} and Ni^{3+} ions. At 210 °C, the reaction between NiOOH and Ag_2O at a NaOH concentration of 2.0 M in the present study yields phase-pure 2H- and 3R-$AgNiO_2$, as determined by PXD. Indeed, by increasing the reaction temperature over the previous synthesis the crystallinity of the 3R-$AgNiO_2$ product was significantly increased (Figure 9). Under similar conditions, as expected, no $CuNiO_2$ was observed since a redox reaction occurred between Cu_2O and NiOOH to form the divalent oxides, CuO and NiO.

Rhodium. Little has been reported on the aqueous solubility of Rh_2O_3 and $Rh(OH)_3$ because of the rarity and high cost of the metal. Using both titrations and colorimetry measurements, Ivanov-Emin et al. investigated the solubility of hydrated Rh_2O_3 at room temperature and reported a maximum solubility of $[Rh^{3+}] \approx 0.01$ mol/L at a hydroxide

concentration of 11 M.[124] At sodium hydroxide concentrations similar to the present experimental conditions (<2.5 M), the solubility of Rh^{3+} is $[Rh^{3+}] \approx 10^{-4}$ mol/L, a value comparable to that of Sc^{3+} and consistent with rhodium oxides being classified as weakly amphoteric. The solubility of $Rh(OH)_3$ results in the formation of both 3R-$CuRhO_2$ and 3R-$AgRhO_2$ at 210 °C and a hydroxide concentration of 2.5 M via reaction of Cu_2O or Ag_2O, respectively, with $Rh(OH)_3$.

5. Conclusions

The formation of delafossite-type oxides accessed by a single step, low temperature (<210 °C) and low pressure (<20 atm) hydrothermal synthetic route has been examined. Solubility data and Eh−pH diagrams for each metal oxide afford phase-pure products and insight into why certain delafossite-type oxides form and why a few others do not. We observe that for a successful delafossite synthesis a necessary condition is that both the component A-site and B-site metal oxides reach a minimum solubility. Primarily, this can be estimated from the acid−base character of the metal oxide. Only metal oxides with some acidic character dissolve and therefore form delafossite-type oxides; basic metal oxides remained as insoluble trihydroxides. For metals with weak acidic character, the mass yield of the delafossite-type oxide product is increased with greater hydroxide mineralizer concentration. With respect to reactant selection, it is also important to avoid metal oxides that form a passivating layer, which slows and/or prevents dissolution of the reactant and therefore limits product formation. Indeed, with each of these factors, the geochemical, environmental, and corrosion science literature on aqueous metal oxide chemistry are an invaluable resource to improve the understanding and synthetic utility of hydrothermal reactions and to move away from empiricism.

Acknowledgment. The authors would like to thank our coworkers D. Shahriari and M. Sasaki who have contributed to the synthesis of delafossite-type oxides. The authors gratefully acknowledge support from the Department of Energy, National Renewable Energy Laboratory Subcontract (Award No. XAT-5-33636-02), and the MRSEC program of the National Science Foundation (Grant DMR-0076097). The authors made use of Central Facilities supported by the MRSEC program of the National Science Foundation (Grant DMR-0076097) at the Materials Research Center of Northwestern University. The SEM work was performed by M. Russell and S. DiBenedetto in the EPIC facility of NUANCE Center at Northwestern University. The NUANCE Center is supported by NSF-NSEC, NSF-MRSEC, Keck Foundation, the State of Illinois, and Northwestern University. W.C.S was additionally supported through a Natural Science and Engineering Research Council of Canada (NSERC) Julie-Payette post-graduate scholarship.

Supporting Information Available: Commercial sources and preparation methods for each B-site constituent metal oxide reagents used (PDF). This material is available free of charge via the Internet at http://pubs.acs.org.

References

(1) Friedel, S. S. *C. R. Acad. Sci. Paris* **1873**, *77*, 211.
(2) Pabst, A. *Am. Mineral.* **1946**, *31*, 539−546.
(3) Soller, W.; Thompson, A. J. *Phys. Rev.* **1935**, *47*, 644.
(4) Staehlin, W.; Oswald, H. R. *Z. Anorg. Allg. Chem.* **1970**, *373*, 69−72.
(5) Prewitt, C. T.; Shannon, R. D.; Rogers, D. B. *Inorg. Chem.* **1971**, *10*, 719−723.
(6) Shannon, R. D.; Prewitt, C. T. *Acta Crystallogr., Sect. B* **1969**, *25*, 925−946.
(7) Shannon, R. D. *Acta Crystallogr., Sect. A* **1976**, *A32*, 751−767.
(8) Carcia, P. F.; Shannon, R. D.; Bierstedt, P. E.; Flippen, R. B. *J. Electrochem. Soc.* **1980**, *127*, 1974−1978.
(9) Monnier, J. R.; Hanrahan, M. J.; Apai, G. *J. Catal.* **1985**, *92*, 119−126.
(10) Christopher, J.; Swamy, C. S. *J. Mater. Sci.* **1992**, *27*, 1353−1356.
(11) Domen, K.; Ikeda, S.; Takata, T.; Tanaka, A.; Hara, M.; Kondo, J. N. *Appl. Energy* **2000**, *67*, 159−179.
(12) Bessekhouad, Y.; Trari, M.; Doumerc, J. P. *Int. J. Hydrogen Energy* **2003**, *28*, 43−48.
(13) Doumerc, J. P.; Parent, C.; Chao, Z. J.; Le Flem, G.; Ammar, A. *J. Less-Common Met.* **1989**, *148*, 333−337.
(14) Jacob, A.; Parent, C.; Boutinaud, P.; Le Flem, G.; Doumerc, J. P.; Ammar, A.; Elazhari, M.; Elaatmani, M. *Solid State Commun.* **1997**, *103*, 529−532.
(15) Nagaura, T. *Prog. Batteries Solar Cells* **1982**, *4*, 105−107.
(16) Benko, F. A.; Koffyberg, F. P. *J. Phys. Chem. Solids* **1984**, *45*, 57−59.
(17) Kawazoe, H.; Yasukawa, M.; Hyodo, H.; Kurita, M.; Yanagi, H.; Hosono, H. *Nature (London)* **1997**, *389*, 939−942.
(18) Yanagi, H.; Hase, T.; Ibuki, S.; Ueda, K.; Hosono, H. *Appl. Phys. Lett.* **2001**, *78*, 1583−1585.
(19) Rogers, D. B.; Shannon, R. D.; Prewitt, C. T.; Gillson, J. L. *Inorg. Chem.* **1971**, *10*, 723−727.
(20) Tanaka, M.; Hasegawa, M.; Higuchi, T.; Tsukamoto, T.; Tezuka, Y.; Shin, S.; Takei, H. *Physica B* **1998**, *245*, 157−163.
(21) Shannon, R. D.; Rogers, D. B.; Prewitt, C. T. *Inorg. Chem.* **1971**, *10*, 713−718.
(22) Krause, A.; Gawryck, S. *Z. Anorg. Allg. Chem.* **1938**, *238*, 406−412.
(23) Croft, W. J.; Tombs, N. C.; England, R. E. *Acta Crystallogr.* **1964**, *17*, 313.
(24) Doumerc, J. P.; Ammar, A.; Wichainchai, A.; Pouchard, M.; Hagenmuller, P. *J. Phys. Chem. Solids* **1987**, *48*, 37−43.
(25) Wichainchai, A.; Dordor, P.; Doumerc, J. P.; Marquestaut, E.; Pouchard, M.; Hagenmuller, P.; Ammar, A. *J. Solid State Chem.* **1988**, *74*, 126−131.
(26) Shin, Y. J.; Doumerc, J. P.; Pouchard, M.; Hagenmuller, P. *Mater. Res. Bull.* **1993**, *28*, 159−165.
(27) Shimode, M.; Sasaki, M.; Mukaida, K. *J. Solid State Chem.* **2000**, *151*, 16−20.
(28) Park, S.; Keszler, D. A. *J. Solid State Chem.* **2003**, *173*, 355−358.
(29) Koehler, B. U.; Jansen, M. *Z. Kristallogr.* **1983**, *165*, 313−314.
(30) Koehler, B. U.; Jansen, M. *J. Solid State Chem.* **1987**, *71*, 566−569.
(31) Rabenau, A. *Angew. Chem., Int. Ed. Engl.* **1985**, *24*, 1026−1040 and references therein.
(32) Whittingham, M. S.; Guo, J.-D.; Chen, R.; Chirayil, T.; Janauer, G.; Zavalij, P. *Solid State Ionics* **1995**, *75*, 257−268.
(33) Walton, R. I. *Chem. Soc. Rev.* **2002**, *31*, 230−238.
(34) Rabenau, A.; Rau, H. *Philips Tech. Rev.* **1969**, *30*, 89−96.
(35) Toedheide, K. In *Water: a Comprehensive Treatise, Vol. 1*; Franks, F., Ed.; Plenum: New York, 1972; pp 463−514.
(36) Seward, T. M. *Phys. Chem. Earth* **1981**, *13*−*14*, 113−132.
(37) Baes, C. F., Jr.; Mesmer, R. E. *The Hydrolysis of Cations*; Krieger Publishing Company: Malabar, FL, 1976.
(38) Brown, G. E., Jr.; Henrich, V. E.; Casey, W. H.; Clark, D. L.; Eggleston, C.; Felmy, A.; Goodman, D. W.; Graetzel, M.; Maciel, G.; McCarthy, M. I.; Nealson, K. H.; Sverjensky, D. A.; Toney, M. F.; Zachara, J. M. *Chem. Rev.* **1999**, *99*, 77−174.
(39) Wesolowski, D. J.; Ziemniak, S. E.; Anovitz, L. M.; Machesky, M. L.; Benezeth, P.; Palmer, D. A. In *Aqueous Systems at Elevated Temperatures and Pressures: Physical chemistry in water, steam and hydrothermal solutions*; Palmer, D. A., Fernandez-Prini, R., Harvey, A. H., Eds.; Academic Press: New York, 2004; pp 493−595.
(40) Misra, C. *Industrial Alumina Chemicals*; American Chemical Society Monograph Series, Vol. 184; American Chemical Society: Washington, DC, 1986.
(41) Diakonov, I. I.; Pokrovski, G. S.; Benezeth, P.; Schott, J.; Dandurand, J.-L.; Escalier, J. *Geochim. Cosmochim. Acta* **1997**, *61*, 1333−1343.
(42) Krylov, O. V. *Catalysis by Nonmetals: Rules for Catalyst Selection*; Physical Chemistry, a Series of Monographs, Vol. 17; Academic Press: New York, 1970.
(43) Cotton, F. A.; Wilkinson, G.; Bochmann, M.; Murillo, C. *Advanced Inorganic Chemistry*, 6th ed.; John Wiley: New York, 1998.
(44) Phillips, C. S. G.; Williams, R. J. P. *Inorganic Chemistry, Vol. 1: Principles and Non-Metals*; Oxford University Press: Oxford, 1965.
(45) Lewis, J. I. *Sch. Sci. Rev.* **1981**, *63*, 128−130.
(46) Smith, D. W. *J. Chem. Educ.* **1987**, *64*, 480−481.
(47) Lewis, J. I.; Anthony, C. *Educ. Chem.* **1986**, *23*, 116−118.
(48) Pourbaix, M. *Thermodynamique des solutions aqueuses dilluees. Representation graphique du role du pH et du potentiel*; Meinema: Delft, 1945; English translation by J. N. Agnar, Arnold, London, 1949.
(49) Pourbaix, M. *Atlas of Electrochemical Equilibria in Aqueous Solutions*; Pergamon Press: New York, 1966.
(50) Garrels, R. M.; Christ, C. L. *Solutions, Minerals, and Equilibria*; Harper's Geoscience Series; Harper and Row: New York, 1965.

(51) Barnum, D. W. *J. Chem. Educ.* **1982**, *59*, 809−812.
(52) Beverskog, B.; Puigdomenech, I. *Corros. Sci.* **1996**, *38*, 2121−2135.
(53) Pourbaix, M. *Rapp. Tech. Cent. Belge Etude Corros.* **1982**, *142*, 101−115.
(54) Halasyamani, P.; Willis, M. J.; Stern, C. L.; Poeppelmeier, K. R. *Inorg. Chem.* **1996**, *35*, 1367−1371.
(55) Harrison, W. T. A.; Dussack, L. L.; Jacobson, A. J. *J. Solid State Chem.* **1996**, *125*, 234−242.
(56) Doran, M. B.; Norquist, A. J.; O'Hare, D. *Inorg. Chem.* **2003**, *42*, 6989−6995.
(57) Gier, T. E.; Stucky, G. D. *Nature (London)* **1991**, *349*, 508−510.
(58) Halasyamani, P.; Willis, M. J.; Stern, C. L.; Poeppelmeier, K. R. *Inorg. Chim. Acta* **1995**, *240*, 109−115.
(59) Emons, H. H.; Beger, E. *Wiss. Z. Tech. Hochsch. Chem. Leuna-Merseburg* **1967**, *9*, 256−260.
(60) Martell, A. E.; Hancock, R. D. *Metal Complexes in Aqueous Solutions*; Plenum: New York, 1996.
(61) Palmer, D. A.; Benezeth, P.; Wesolowski, D. J. *Geochim. Cosmochim. Acta* **2001**, *65*, 2081−2095.
(62) Kamau, P.; Jordan, R. B. *Inorg. Chem.* **2001**, *40*, 3879−3883.
(63) Schwertmann, U.; Cornell, R. M. *Iron Oxides in the Laboratory*, 2nd ed.; Wiley-VCH: Weinheim, 2000.
(64) Amatucci, G. G.; Tarascon, J. M.; Larcher, D.; Klein, L. C. *Solid State Ionics* **1996**, *84*, 169−180.
(65) Sac-Epee, N.; Palacin, M. R.; Beaudoin, B.; Delahaye-Vidal, A.; Jamin, T.; Chabre, Y.; Tarascon, J. M. *J. Electrochem. Soc.* **1997**, *144*, 3896−3907.
(66) Allen, J. L.; Poeppelmeier, K. R. *Polyhedron* **1994**, *13*, 1301−1310.
(67) Noerlund Christensen, A. *Acta Chem. Scand. (1947−1973)* **1967**, *21*, 121−126.
(68) *Jade*, 5.0 edition; Materials Data Inc.: Livermore, CA, 1999.
(69) *PowderCell*, Version 2.4; Federal Institute for Materials Research and Testing: Berlin, Germany, 2000.
(70) Otabe, T.; Ueda, K.; Kudoh, A.; Hosono, H.; Kawazoe, H. *Appl. Phys. Lett.* **1998**, *72*, 1036−1038.
(71) Tate, J.; Jayaraj, M. K.; Draeseke, A. D.; Ulbrich, T.; Sleight, A. W.; Vanaja, K. A.; Nagarajan, R.; Wager, J. F.; Hoffman, R. L. *Thin Solid Films* **2002**, *411*, 119−124.
(72) Shin, Y. J.; Doumerc, J. P.; Dordor, P.; Pouchard, M.; Hagenmuller, P. *J. Solid State Chem.* **1993**, *107*, 194−200.
(73) Clayton, J. E.; Cann, D. P.; Ashmore, N. *Thin Solid Films* **2002**, *411*, 140−146.
(74) Attili, R. N.; Uhrmacher, M.; Lieb, K. P.; Ziegeler, L.; Mekata, M.; Schwarzmann, E. *Phys. Rev. B: Condens. Matter* **1996**, *53*, 600−608.
(75) Shahriari, D. Y.; Erdman, N.; Haug, U. T. M.; Zarzyczny, M. C.; Marks, L. D.; Poeppelmeier, K. R. *J. Phys. Chem. Solids* **2003**, *64*, 1437−1441.
(76) Latimer, W. M. *The Oxidation States of the Elements and Their Potentials in Aqueous Solutions*, 2nd ed.; Prentice Hall: New York, 1964.
(77) Kolthoff, I. M.; Coetzee, J. F. *J. Am. Chem. Soc.* **1957**, *79*, 9, 1852−1858.
(78) Var′yash, L. N.; Rekharskii, V. I. *Geokhimiya* **1981**, 683−688.
(79) Var′yash, L. N.; Rekharskii, V. I. *Geokhimiya* **1981**, 1003−1008.
(80) Beverskog, B.; Puigdomenech, I. *J. Electrochem. Soc.* **1997**, *144*, 3476−3483.
(81) Johnston, H. L.; Cuta, F.; Garrett, A. B. *J. Am. Chem. Soc.* **1933**, *55*, 2311−2325.
(82) Kozlov, V. K.; Kuznetsov, V. N.; Khodakovskii, I. L. *Geokhimiya* **1983**, 215−227.
(83) Nikolaeva, N. M.; Pogodina, L. P.; Malkova, V. I. *Zh. Neorg. Khim.* **1985**, *30*, 1059−1063.
(84) Pound, B. G.; Macdonald, D. D.; Tomlinson, J. W. *Electrochim. Acta* **1979**, *24*, 929−937.
(85) Haas, H.; Kordes, E. *Z. Kristallogr.* **1969**, *129*, 259−270.
(86) Koehler, B. U.; Jansen, M. *Z. Anorg. Allg. Chem.* **1986**, *543*, 73−80.
(87) Ivanov-Emin, B. N.; Nisel'son, L. A.; Ivolgina, A. T. *Zh. Neorg. Khim.* **1960**, *5*, 2841−2842.
(88) Ivanov-Emin, B. N.; Nisel'son, L. A.; Ivolgina, A. T. *Zh. Inorg. Khim.* **1961**, *6*, 1483−1484.
(89) Deberdt, S.; Castet, S.; Dandurand, J.-L.; Harrichoury, J.-C.; Louiset, I. *Chem. Geol.* **1998**, *151*, 349−372.
(90) Delorme, C. *Acta Crystallogr.* **1956**, *9*, 200.
(91) Kuyunko, N. S.; Malinin, S. D.; Khodakovskii, I. L. *Geokhimiya* **1983**, 419−428.
(92) Bourcier, W. L.; Knauss, K. G.; Jackson, K. J. *Geochim. Cosmochim. Acta* **1993**, *57*, 747−762.
(93) Castet, S.; Dandurand, J. L.; Schott, J.; Gout, R. *Geochim. Cosmochim. Acta* **1993**, *57*, 4869−4884.
(94) Shahriari, D. Y.; Barnabe, A.; Mason, T. O.; Poeppelmeier, K. R. *Inorg. Chem.* **2001**, *40*, 5734−5735.
(95) Ivanov-Emin, B. N.; Rabovik, Y. I. *Zh. Obshch. Khim.* **1944**, *14*, 781−785.
(96) Ivanov-Emin, B. N.; Nisel'son, L. A.; Larionova, L. E. *Zh. Neorg. Khim.* **1962**, *7*, 522−526.
(97) Thompson, L. C. A.; Pacer, R. *J. Inorg. Nucl. Chem.* **1963**, *25*, 1041−1044.
(98) Aksel'rud, N. V.; Spivakovskii, V. B. *Zh. Anal. Khim.* **1957**, *12*, 75−79.
(99) Ivanov-Emin, B. N.; Ostroumov, E. A. *Zh. Obshch. Khim.* **1947**, *17*, 1595.
(100) Ivanov-Emin, B. N.; Nisel'son, L. A.; Greksa, Y. *Zh. Neorg. Khim.* **1960**, *5*, 1996−1998.
(101) Ivanov-Emin, B. N.; Rybina, V. I.; Kornev, V. I. *Zh. Neorg. Khim.* **1965**, *10*, 1005−1008.
(102) Rai, D.; Sass, B. M.; Moore, D. A. *Inorg. Chem.* **1987**, *26*, 345−349.
(103) Beverskog, B.; Puigdomenech, I. *Corros. Sci.* **1997**, *39*, 43−57.
(104) Ziemniak, S. E.; Jones, M. E.; Combs, K. E. S. *J. Solution Chem.* **1998**, *27*, 33−66.
(105) L'Vov, B. V. *Thermochim. Acta* **1999**, *333*, 13−19.
(106) Li, J.; Fisher, C. L.; Chen, J. L.; Bashford, D.; Noodleman, L. *Inorg. Chem.* **1996**, *35*, 4694−4702.
(107) Chouaib, F.; Heubel, P. H.; Del Carmen Sanson, M.; Picard, G.; Tremillon, B. *J. Electroanal. Chem. Interfacial Electrochem.* **1981**, *127*, 179−193.
(108) Toepfer, J.; Trari, M.; Gravereau, P.; Chaminade, J. P.; Doumerc, J. P. *Z. Kristallogr.* **1995**, *210*, 184−187.
(109) Feng, Q.; Kanoh, H.; Miyai, Y.; Ooi, K. *Chem. Mater.* **1995**, *7*, 1226−1232.
(110) Lengweiler, H.; Buser, W.; Feitknecht, W. *Helv. Chim. Acta* **1961**, *44*, 796−805.
(111) Lengweiler, H.; Buser, W.; Feitknecht, W. *Helv. Chim. Acta* **1961**, *44*, 805−811.
(112) Kamnev, A. A.; Ezhov, B. B.; Malandin, O. G.; Vasev, A. V. *Zh. Prikl. Khim.* **1986**, *59*, 1689−1693.
(113) Diakonov, I. I.; Schott, J.; Martin, F.; Harrichourry, J. C.; Escalier, J. *Geochim. Cosmochim. Acta* **1999**, *63*, 2247−2261.
(114) Sergeeva, E. I.; Suleimenov, O. M.; Evstigneev, A. V.; Khodakovsky, I. L. *Geokhimiya* **1999**, 1218−1229.
(115) Feitknecht, W.; Moser, K. *Z. Anorg. Allg. Chem.* **1960**, *304*, 181−184.
(116) Cubicciotti, D. *Corrosion* **1988**, *44*, 875−880.
(117) Macdonald, D. D.; Shierman, G. R.; Butler, P. *Thermodynamics of metal-water systems at elevated temperatures. 3. Cobalt-water system*; Whiteshell Nuclear Research Establishment, Atomic Energy Canada Limited: Pinawa, MB, Canada 1972.
(118) Rotinyan, A. L.; Kheifets, V. L.; Nikolaeva, S. A. *Zh. Neorg. Khim.* **1961**, *6*, 21−26.
(119) Ezhov, B. B.; Kamnev, A. A. *Zh. Prikl. Khim.* **1983**, *56*, 2346−2348.
(120) Balej, J.; Divisek, J. *Collect. Czech. Chem. Commun.* **1997**, *62*, 1663−1676.
(121) Emons, H. H.; Beger, E. *Z. Chem.* **1967**, *7*, 200−201.
(122) Staehlin, W.; Oswald, H. R. *Z. Anorg. Allg. Chem.* **1969**, *367*, 206−208.
(123) Beverskog, B.; Puigdomenech, I. *Corros. Sci.* **1997**, *39*, 969−980.
(124) Ivanov-Emin, B. N.; Borzova, L. D.; Egorov, A. M.; Malyugina, S. G. *Zh. Neorg. Khim.* **1971**, *16*, 2766−2768.

CM051791C